Journal of Visualized Experiments

An experimental method to uncouple effects of Coriolis force and rotating buoyancy on full-field heat transfer properties of a rotating channel

--Manuscript Draft--

Article Type:	Invited Methods Article - JoVE Produced Video
Manuscript Number:	JoVE57630R3
Full Title:	An experimental method to uncouple effects of Coriolis force and rotating buoyancy on full-field heat transfer properties of a rotating channel
Keywords:	Rotating Channel Flow, Heat Convection, Gas Turbine Rotor Blade Cooling, Orthogonal Mode Rotation, Coriolis Effect, Rotating Buoyancy Effect.
Corresponding Author:	Shyy Woei Chang National Cheng Kung University Tainan, TAIWAN
Corresponding Author's Institution:	National Cheng Kung University
Corresponding Author E-Mail:	swchang@mail.ncku.edu.tw
First Author:	Shyy Woei Chang
Other Authors:	Hong-Da Shen
	Kuo-Ching Yu
	W.-L. Cai
Author Comments:	Thank you for the editorial efforts to carefully review this article. We have fully responded the comments and made the according modifications and corrections.
Additional Information:	
Question	**Response**
If this article needs to be "in-press" by a certain date, please indicate the date below and explain in your cover letter.	

To: Dr. Phillip Steindel
Review Editor, JoVE.

Re: Revised JoVE57630 R2
An experimental method to uncouple effects of Coriolis force and rotating buoyancy on full-field heat transfer property of a rotating channel.

Dear Editor Steindel,

Thank you for arranging the review of our work.

We have fully responded all the editorial comments provided. I have invited my friend in Austria, Dr. Andrew Neeson, to improve the English.

The locations with English improvements are indicated by the red bars at the numbers of the sentences. The modifications and corrections for the rest of editorial comments are indicated as the pink prints in the revised manuscript.

Once again, thank you for the kind considerations. We look forward to hearing from you soon.

Best wishes.

Shyy Woei Chang
Professor,
Department of System and Naval Mechatronic Engineering,
National Cheng Kung University.

TITLE:

Uncoupling Coriolis Force and Rotating Buoyancy Effects on Full-Field Heat Transfer Properties of a Rotating Channel

AUTHORS & AFFILIATIONS:

Shyy Woei Chang, Wei-Ling Cai, Hong-Da Shen, Kuo-Ching Yu

Department of System and Naval Mechatronic Engineering, National Cheng Kung University, Taiwan R.O.C.

Corresponding Author:

Shyy Woei Chang (swchang@mail.ncku.edu.tw)

Email Addresses of Co-authors:

Wei-Ling Cai (992232024@stu.nkmu.edu.tw)

Hong-Da Shen (harry903208888@yahoo.com.tw)

Kuo-Ching Yu (yugojim@gmail.com)

KEYWORDS:

Rotating Channel Flow, Heat Convection, Gas Turbine Rotor Blade Cooling, Orthogonal Mode Rotation, Coriolis Effect, Rotating Buoyancy Effect.

SHORT ABSTRACT:

Here, we present an experimental method for decoupling the interdependent Coriolis-force and rotating-buoyancy effects on full-field heat transfer distributions of a rotating channel.

LONG ABSTRACT:

An experimental method for exploring the heat transfer characteristics of an axially rotating channel is proposed. The governing flow parameters that characterize the transport phenomena in a rotating channel are identified via the parametric analysis of the momentum and energy equations referring to a rotating frame of reference. Based on these dimensionless flow equations, an experimental strategy that links the design of the test module, the experimental program and the data analysis is formulated with the attempt to reveal the isolated Coriolis-force and buoyancy effects on heat transfer performances. The effects of Coriolis force and rotating buoyancy are illustrated using the selective results measured from rotating channels with various geometries. While the Coriolis-force and rotating-buoyancy impacts share several common features among the various rotating channels, the unique heat transfer signatures are found in association with the flow direction, the channel shape and the arrangement of heat transfer enhancement devices. Regardless of the flow configurations of the rotating channels, the presented experimental method enables the development of physically consistent heat transfer correlations that permit the evaluation of isolated and interdependent Coriolis-force and rotating-buoyancy effects on the heat transfer properties of rotating channels.

INTRODUCTION:

While thermodynamic laws dictate the improved specific power and thermal efficiency of a gas turbine engine by elevating the turbine entry temperature, several hot engine components, such as turbine blades, are prone to thermal damage. Internal cooling of a gas turbine rotor blade permits a turbine entry temperature in excess of the temperature limits of the creep resistance of the blade material. However, the configurations of the internal cooling channels must comply with the blade profile. In particular, the coolant rotates within the rotor blade. With such harsh thermal conditions for a running gas turbine rotor blade, an effective blade cooling scheme is crucial to ensure the structure's integrity. Thus, the local heat transfer properties for a rotating channel are important for the efficient usage of the limited coolant flow available. The acquisition of useful heat transfer data that are applicable to the design of the internal coolant passages at realistic engine conditions is of primary importance when an experimental method is developed for measuring the heat transfer properties of a simulated cooling passage inside a gas turbine rotor blade.

Rotation at a speed above 10,000 rpm considerably alters the cooling performance of a rotating channel inside a gas turbine rotor blade. The identification of engine conditions for such a rotating channel is permissible using the similarity law. With rotation, the dimensionless groups that control the transport phenomena inside a radially rotating channel can be revealed by deriving the flow equations relative to a rotating frame of reference. Morris[1] has derived the momentum conservation equation of flow relative to a rotating frame of reference as:

$$\frac{\mathrm{D}\bar{v}}{\mathrm{D}t} + 2(\omega \times \bar{v}) - \beta\left(T - T_{ref}\right)(\omega \times \omega \times \bar{r}) = -\frac{1}{\rho_{ref}}\nabla P^{*} + \nu\nabla^{2}\bar{v} \qquad (1)$$

In equation (1), the local fluid velocity, $\bar{v}$, with the position vector, $\bar{r}$, relative to a frame of reference rotating at the angular velocity, ω, is affected by the Coriolis acceleration in terms of $2(\omega\times\bar{v})$, the decoupled centripetal buoyancy force, $\beta(T\text{-}T_{ref})(\omega\times\omega\times\bar{r})$, the driven piezo-metric pressure gradient, ∇P^{*}, and the fluid dynamic viscosity, ν. The referenced fluid density, ρ_{ref}, is referred to a pre-defined fluid reference temperature T_{ref}, which is typical of the local fluid bulk temperature for experiments. If the irreversible conversion of mechanical energy into thermal energy is negligible, the energy conservation equation is reduced to:

$$\rho C_{p}\frac{\mathrm{D}T}{\mathrm{D}t} = k_{f}\nabla^{2}T \qquad (2)$$

The first term of equation (2) is obtained by treating the specific enthalpy to be directly related to the local fluid temperature, T, via the constant specific heat, C_p. As the perturbation of fluid density caused by the variation of fluid temperature in a heated rotating channel provides considerable influence on the motion of fluids when it links with the centripetal acceleration in equation (1), the fluid velocity and temperature fields in an axially rotating channel are coupled. Also, both Coriolis and centripetal accelerations vary simultaneously as the rotating speed is adjusted. Thus, the effects of Coriolis force and rotating buoyancy on the fields of fluid velocity and temperature are naturally coupled.

Equations (1) and (2) in the dimensionless forms disclose the flow parameters that govern the

heat convection in a rotating channel. With a basically uniform heat flux imposed on a rotating channel, the local fluid bulk temperature, T_b, increases linearly in the streamwise direction, s, from the reference inlet level, T_{ref}. The local fluid bulk temperature is determined as $T_{ref} + \tau s$, where τ is the gradient of the fluid bulk temperature in the direction of flow. Substitutions of the following dimensionless parameters of:

$$\vec{V} = \bar{v}/V_{mean} \quad (3) \qquad \Omega = \omega/N \quad (4)$$

$$\vec{R} = \bar{r}/d \quad (5)$$

$$\lambda = P^*/(\rho_{ref} V_{mean}^2) \quad (6)$$

$$\eta = (T - T_{ref})/(\tau d) \quad (7)$$

into equations (1) and (2), where V_{mean}, N and d respectively stand for the mean flow through velocity, rotating velocity and channel hydraulic diameter, the dimensionless flow momentum and energy equations are derived as equations (8) and (9) respectively.

$$\frac{\mathrm{D}\vec{V}}{\mathrm{D}t} + Ro\left(2\Omega \times \vec{V}\right) - Ro^2 \beta \tau d \eta \left(\Omega \times \Omega \times \vec{R}\right) = -\nabla\lambda + \frac{1}{Re}\nabla^2\vec{V} \quad (8)$$

$$\frac{\mathrm{D}\eta}{\mathrm{D}t} = \frac{1}{RePr}\nabla^2\eta \quad (9)$$

Evidently, η in equation (9) is a function of Re, Ro, and $Bu = Ro^2 \beta \tau d R$, which are respectively referred to as Reynolds, rotation and buoyancy numbers. The Rossby number that quantifies the ratio between inertial and Coriolis forces is equivalent to the inverse rotation number in equation (8).

When T_b is calculated as $T_{ref} + \tau s$ in a rotating channel subject to a uniform heat flux, the τ value can be alternatively evaluated as $Q_f/(mC_pL)$ in which Q_f, m and L are the convective heating power, coolant mass flow rate and channel length, respectively. Thus, the dimensionless local fluid bulk temperature, η_b, is equal to s/d and the dimensionless temperature at channel wall, η_w, yields $[(T_w\text{-}T_b)/Q_f][mC_p][L/d]+s/d$. With the convective heat transfer rate defined as $Q_f/(T_w\text{-}T_b)$, the dimensionless wall-to-fluid temperature difference, $\eta_w\text{-}\eta_b$, is convertible into the local Nusselt number via equation (10) in which ζ is the dimensionless shape function of heating area and channel sectional area.

$$Nu(s) = \zeta \frac{RePr}{\eta_w(s) - \eta_b(s)} \quad (10)$$

With a set of predefined geometries and the hydrodynamic and thermal boundary conditions, the dimensionless groups controlling the local Nusselt number of a rotating channel are identified as:

$$Re = V_{mean} d/v \quad (11)$$

$$Ro = Nd/V_{mean} \quad (12)$$

$$Bu = Ro^2 \beta \tau d R \quad (13)$$

With experimental tests, the adjustment of rotating speed, *N*, for varying *Ro* to generate the heat transfer data at different strengths of Coriolis forces inevitably changes the centripetal acceleration, and thus, the relative strength of rotating buoyancy. Moreover, a set of heat transfer data collected from a rotating channel is always subject to a finite degree of rotating buoyancy effect. To disclose the individual effects of Coriolis-force and buoyancy on the heat transfer performance of a rotating channel requires the uncoupling of the *Ro* and *Bu* effects on *Nu* properties through the post data processing procedure that is inclusive in the present experimental method.

The engine and laboratory flow conditions for a rotating channel inside a gas turbine rotor blade can be specified by the ranges of *Re*, *Ro* and *Bu*. The typical engine conditions for the coolant flow through a gas turbine rotor blade, as well as the construction and commissioning of the rotating test facility that allowed experiments to be performed near the actual engine conditions was reported by Morris[2]. Based on the realistic engine conditions summarized by Morris[2], **Figure 1** constructs the realistic operating conditions in terms of *Re*, *Ro* and *Bu* ranges for a rotating coolant channel in a gas turbine rotor blade. In **Figure 1**, the indication of an engine's worst condition is referred to as the engine running condition at the highest rotor speed and the highest density ratio. In **Figure 1**, the lower limit and worst engine operating conditions respectively emerge at the lowest and highest engine speeds. It is extremely difficult to measure the full-field *Nu* distribution of a rotating channel running at a real engine speed between 5000 and 20,000 rpm. However, based on the similarity law, laboratory-scale tests have been conducted at reduced rotating speeds but with several attempts to provide a full coverage of the real-engine *Re*, *Ro* and *Bu* ranges. As an innovative experimental method, the NASA HOST program[3-6] adopted the high-pressure tests for increasing the fluid densities at the predefined *Re* in order to extend the *Ro* range by reducing the mean fluid velocity. In this regard, the specific relationships between *Re*, *Ro* and *Bu* for an ideal gas with a gas constant, R_c, and viscosity, μ, are related as:

$$Ro = Re^{-1}(Pd^2N)/(R_c T_b \mu) \quad (14)$$

$$Bu = Ro^2 R(T_w - T_b)/T_b \quad (15)$$

To bring the laboratory conditions into the nominal correspondence with engine conditions seen in **Figure 1**, the rotating speed, *N*, coolant pressure, *P*, channel hydraulic diameter, *d*, rotating radius, *R*, and wall-to-fluid temperature difference, T_w-T_b, need to be controlled for matching the realistic *Re*, *Ro* and *Bu* ranges. Clearly, one of the most effective approaches to extend the *Ro* range is to increase channel hydraulic diameter, as *Ro* is proportional to d^2. As the laboratory heat transfer test at realistic *N* is extremely difficult, the coolant pressure, *P*, is technically easier to be raised for extending *Ro* range; even if *Ro* is only proportional to *P*. Based on this theoretical background, the design philosophy of the present experimental method is to increase *Ro* by pressurizing the rotating test channel using the maximum channel hydraulic diameter allowed to fit into the rotating rig. Having increased the *Ro* range, the range of *Bu* is accordingly extended as *Bu* is proportional to Ro^2. In **Figure 1**, the laboratory test conditions adopted to generate the

heat transfer data of rotating channels are also included[3-29]. As indicated in **Figure 1**, the coverage of realistic engine conditions by the available heat transfer data is still limited, especially for the required *Bu* range. The open and the colored solid symbols depicted in **Figure 1** are the pointed and full-field heat transfer experiments, respectively. As collected in **Figure 1**, most of the heat transfer data with cooling applications to gas turbine rotor blades[1-18,20-26] are point measurements using the thermocouple method. The wall conduction effects on measuring the wall conductive heat flux and the temperatures at fluid-wall interfaces undermine the quality of heat transfer data converted from the thermocouple measurements. Also, the heat transfer measurements[1-18,20-26] using the thermocouple method cannot detect the two-dimensional heat transfer variations over a rotating surface. With the present experimental method[29-32], the detection of full-field Nusselt number distributions over the rotating channel wall is permissible. The minimization of wall conduction effect using 0.1 mm thick stainless-steel foils with Biot numbers >>1 to generate the heating power by the present experimental method permits the one-dimensional heat conduction from the heating foil to the coolant flow. In particular, the acquisition of full-field heat transfer data involving both *Ro* and *Bu* effects is not permissible using the transient liquid crystal technique and the thermocouple method. With the current steady-state liquid crystal thermography method[19], the detectable temperature range of 35-55 °C disables the generation of heat transfer data with realistic density ratios.

Using the flow parameters governing the heat convection in a rotating channel to demonstrate that the full coverage of realistic engine conditions seen in **Figure 1** has not yet been achieved, so the need for acquiring the full-field heat transfer data at realistic engine conditions has been continuously urged. The present experimental method enables the generation of full-field heat transfer with both Coriolis-force and rotating-buoyancy effects detected. The protocols are aimed at assisting the investigators to devise an experimental strategy relevant to the realistic full-field heat transfer measurement of a rotating channel. Along with the method of parametric analysis that is unique to the present experimental method, the generation of heat transfer correlation for assessing the isolated and interdependent *Ro* and *Bu* effects on *Nu* is permitted.

The article illustrates an experimental method aimed at generating the two-dimensional heat transfer data of a rotating channel with flow conditions similar to the realistic gas turbine engine conditions but operating at much lower rotating speeds in the laboratories. The method developed to select the rotating speed, the hydraulic diameter of test channel and the range of wall-to-fluid temperature differences for acquiring the heat transfer data at realistic engine conditions is illustrated in the introduction. The calibration tests for the infrared thermography system, the heat loss calibration tests and the operation of the rotating heat transfer test rig are shown. The factors causing the significant uncertainties for heat transfer measurements and the procedures for decoupling the Coriolis-force and buoyancy effects on the heat transfer properties of a rotating channel are described in the article with the selective results to demonstrate the present experimental method.

PROTOCOL:

Note: The details of rotating test facilities, data acquisition, data processing and the heat transfer

test module emulating an internal cooling channel of a gas turbine rotor blade are in our previous works[29-32].

1. Preparation of Heat Transfer Tests

1.1. Formulate the experimental conditions in terms of *Re*, *Ro* and *Bu* from the targeted operation conditions of a gas turbine rotor blade.

1.2. Determine the *N*, *P*, *d*, *R*, and T_w - T_b needed for acquiring the tested *Re*, *Ro* and *Bu* using equations (14) and (15).

1.3. Re-define the targeting *Re*, *Ro* and *Bu* if *N*, *P*, *d*, *R*, and T_w - T_b exceeds the limit of the experimental facilities.

1.4. Design and construct the scaled heat transfer test module emulating a practical internal coolant channel in a gas turbine rotor blade[2].

2. Determination of Thermal Emissivity Coefficient for Infrared Thermography System

2.1. Install the calibrated thermocouple on the back side of the scanned stainless-steel heating foil.

2.2. Spray a thin layer of black paint on the stainless-steel heating foil scanned by the infrared camera.

2.3. Create symmetrical flow fields on two sides of the stainless-steel heating foil by placing a vertical thin stainless-steel foil in a space with the free convective flows over the two sides of the vertical heating foil.

2.4. Feed electrical heating power through the heating foil and measure temperatures simultaneously by thermocouple and infrared thermography system from the computer display at steady state.

2.5. Repeat step 2.4 at least four times using elevated heater powers. Ensure that the wall temperatures corresponding to the heater powers used by steps 2.3 and 2.4 cover the T_w range determined by step 1.2.

2.6. Calculate the T_w values scanned by the infrared thermography system using a number of selective thermal emissivity coefficients for the program that converts the infrared signals into temperature data.

2.7. Compare the T_w data measured by the calibrated thermocouple and the infrared thermography system at the location corresponding to the thermocouple spot with the standard deviations evaluated.

2.8. Select the thermal emissivity coefficient with the minimum standard deviation determined by step 2.7.

2.9. Determine the maximum precision error for the infrared thermography system using the thermal emissivity coefficient determined by step 2.8.

3. Dynamic Balance of Rotating Rig

3.1. Install the heat transfer test module, the infrared camera, the enveloping frame and all accessories on the rotating rig.

3.2. Adjust the counterbalancing weight gradually until the running condition of the rotating rig satisfies the vibrational limitation for the infrared thermographic measurements to exhibit the stable thermal image on the computer display.

4. Evaluation of Heat Loss Coefficients

4.1. Fill the coolant channel of the heat transfer test module with thermal insulation material.

4.2. Install the filled test module on the rotating test rig by fitting the test module on the rotating platform and connecting the heater power supply and all the instrumental cables.

4.3. Activate the data acquisition system to scan the temporal T_w variation at a heating power until the steady state condition is satisfied. Ensure that the temporal T_w variations during several successive scans are less than $\pm$0.3 K at each steady state condition.

4.4. Record the heater power, steady-state T_w data and the corresponding ambient temperature, T_∞.

4.5. Repeat steps 4.3 and 4.4 at least five times using different heating powers at a fixed rotating speed.

4.6. Repeat steps 4.2 - 4.4 with at least five rotating speeds. Ensure that the test range of the rotating speed covers all the *N* values determined by step 1.2.

4.7. Repeat steps 4.3 - 4.6 with a reversed rotating direction.

4.8. Construct the plots of heat loss flux against wall-to-ambient temperature difference at each rotating speed.

4.9. Correlate the heat loss coefficients as the functions of wall-to-ambient temperature difference, rotating speed and direction of rotation.

4.10. Incorporate the heat loss correlation into the post data process program for *Nu* accountancy.

5. Baseline Heat Transfer Tests

5.1. Perform heat transfer tests at the targeting Reynolds numbers at zero rotating speed (*Ro* = *N* = 0) by feeding coolant flows and heater powers to the test module. Ensure the supplied coolant mass flow rate is constantly adjusted in order to control Reynolds number at the flow entry plane at the targeting value.

5.2. Record all the relevant raw data, including the steady state wall temperatures, fluid temperatures, heater powers, flow pressures and ambient pressures and temperatures, for subsequent data processing.

5.3. Evaluate the local and area-averaged Nusselt numbers (Nu_0) over the scanned static channel walls.

6. Rotating Heat Transfer Tests

6.1. Install the on-line monitoring program to monitor the test conditions at the targeting *Re* and *Ro*.

6.2. Feed the measured coolant mass flow rate, airflow pressure, rotating speed and fluid temperature at channel entrance into the monitoring program to calculate the instant *Re* and *Ro*.

6.3. Record all the relevant raw data, such as rotating speed, heater power, airflow and ambient pressures, as well as the wall and fluid temperatures for subsequent data processing after the pre-defined steady-state condition is satisfied.

6.4. Repeat steps 6.2 and 6.3 with at least four ascending or descending heater powers at a set of fixed *Re* and *Ro*. Ensure that the test *Re* and *Ro* fall within ±1% differences from the targeting values by adjusting the rotating speed or the coolant mass flow rate or both.

6.5. Ensure that the heat transfer tests at each set of fixed *Re* and *Ro* with different heater powers are continuously performed as the development of buoyancy induced flows is associated with the "history" of the flow development.

6.6. Repeat steps 6.4 and 6.5 with four or five targeting Reynolds numbers (*Re*) at a fixed rotation number (Ro). Ensure the rotating speed is appropriately adjusted at each test *Re* to control both *Re* and *Ro* at the targeting values within ±1% differences.

6.7. Repeat step 6.6 using four or five targeting rotation numbers (Ro).

6.8. Repeat steps 6.2 to 6.7 with reversed rotating direction.

6.9. Evaluate the local and area-averaged Nusselt numbers (Nu) over the scanned rotating channel walls using a post data processing program.

7. Parametric Analysis

7.1. Correlate the area-averaged Nusselt numbers (Nu_0) collected from the static channel into the functions of Reynolds number.

7.2. Evaluate the full-field local Nu/Nu_0 ratios at each fixed Re and Ro tested with the area-averaged Nu/Nu_0 ratios calculated.

7.3. Verify the applicability of isolation Re effect by plotting the local and area-averaged Nu/Nu_0 ratios obtained with different Re but at identical Ro.

7.4. Disclose the isolated impacts of rotating buoyancy on heat transfer properties of the rotating test channel by plotting the area-averaged Nu/Nu_0 ratios collected at the same Ro with different Re against Bu or density ratio ($\Delta\rho/\rho$). Ensure the preferable selection of Bu or $\Delta\rho/\rho$ to construct this type of plot for obtaining the consistent data trend with a simple functional structure for heat transfer correlation.

7.5. Extrapolate each Nu/Nu_0 data trend collected at a fixed Ro but different Re into the limiting condition of $Bu\rightarrow 0$ or $\Delta\rho/\rho\rightarrow 0$.

7.6. Collect all the extrapolated Nu/Nu_0 results with $Bu\rightarrow 0$ or $\Delta\rho/\rho\rightarrow 0$ at all the tested Ro.

7.7. Plot the extrapolated Nu/Nu_0 results with vanished buoyancy interaction against Ro to disclose the uncoupled Coriolis force effects on the heat transfer properties.

7.8. Correlate the test results collected by steps 7.4 and 7.7 into the functions of Ro and Bu.

REPRESENTATIVE RESULTS:

Realistic operating conditions for the internal coolant flows inside a rotating gas turbine blade in terms of Re, Ro and Bu are compared with the emulated laboratory conditions in **Figure 1**. The data points fall in the realistic engine conditions using the present experimental method summarized in the protocols[11,14,17,20-21]. Although the full-field heat transfer data are more useful than the pointed heat transfer data measured from the rotating channels, most of the previous heat transfer experiments adopt the thermocouple method (**Figure 1**). The present infrared thermography method detects the full-field heat transfer information from a rotating surface with the buoyancy-induced flows fully developed. With the free or forced convective external flows for a static or rotating test channel, the present protocols include the generation of heat loss correlations for post data processing (**Figure 2**). At the top of **Figure 2**, the construction of the heat transfer test module is also demonstrated. The correlative coefficients for all the fitted lines shown by **Figure 2** fall between 0.95-0.98. In view of the h_{loss} correlation seen in the plot of

h_{loss} against N in **Figure 2**, the error bars indicate the data range determined at each rotating speed.

Figures 3-5 depict the selective heat transfer results measured from the static two-pass S-channel with longitudinal wavy ribs, the rotating two-pass S-channel[31] and the rotating furrowed[32] and pin-fin channel[33]. The estimated maximum uncertainties of the *Nu* measurements for the static S-ribbed channel, the rotating S-channel[31], furrowed channel[32] and pin-fin channel[33] are 7.9%, 8.8%, 9.2%, and 9.7%, respectively. To disclose the *Re* impact on the heat transfer properties of a coolant channel, the base-line full-field heat transfer data detected from the static channel by the present infrared thermography method as typified by **Figure 3** are essential. The diagram shown at the top of **Figure 3** also depicts the channel configuration of the two-pass S-channel with the longitudinal wavy ribs. The channel section is square with the semi-circular sectioned longitudinal wavy ribs on two opposite heated walls of the inlet and outlet legs.

The applicability of isolated *Re* impact from *Ro* and *Bu* effects on local and regionally averaged heat transfer is permitted by presenting the heat transfer data in terms of Nu/Nu_0 (**Figure 4**). Both patterns and levels of Nu/Nu_0 at the same *Ro* with similar *Bu* seem to be weak functions of *Re* (**Figure 4**). The typical results from the protocol for disclosing the isolated Coriolis force effects on heat transfer properties are demonstrated in **Figure 5**. In **Figure 5**, the variations of Nu/Nu_0 at each fixed *Ro* against *Bu* for two different rotating channels with wavy endwalls[32] and diamond shaped pin-fins[33] tend to follow linear-like data trends. Thus, the linear extrapolation when $Bu \rightarrow 0$ is selected for the identified Nu/Nu_0 levels at $Bu = 0$ and $Ro > 0$. But, due to the different channel configurations, the Nu/Nu_0 ratios measured from the rotating furrowed[32] and pin-fin[33] channels as depicted in **Figure 5** are respectively decreased and increased by raising *Bu*. In this regard, the depiction of Nu/Nu_0 variations against density ratio ($\Delta\rho/\rho$)[3-6,34] has often led to the non-linear Nu/Nu_0 variations. Thus, the extrapolation of each Nu/Nu_0 data trend at a fixed *Ro* toward the asymptotic limit of $\Delta\rho/\rho \rightarrow 0$ with diminished buoyancy effect along a non-linear data trend is often affected by the type of correlative function selected. Nevertheless, the data extrapolating procedure for the heat transfer results detected from the leading and trailing walls of the rotating channels[32] demonstrates the applicability to unravel the isolated Coriolis force effects on heat transfer properties with vanished buoyancy interaction at $Bu=0$ (**Figure 5**).

The so-called zero-buoyancy Nu/Nu_0 ratios are only controlled by *Ro* to reflect the isolated Coriolis force effects. The manner of heat transfer variations from the static-channel references disclosed by steps 7.7 and 7.8 is typified by **Figure 6**. The separated *Ro* impact from the buoyancy effect on the heat transfer performances of a rotating channel is correlated as the *Ro* function to be a part of Nu/Nu_0 correlation (**Figure 6**). The positive or negative ψ_2 values in **Figure 6** indicate the improving or impeding effects on heat transfer performances due to buoyancy interactions. The larger ψ_2 magnitude, the higher degrees of rotating buoyancy impact are imposed on the heat transfer properties. The fitted lines indicated in **Figure 6** are the plots of the correlative functions. The functional structures of the correlations for zero-buoyancy Nu/Nu_0 ratios and ψ_2 values are generally determined in accordance with the varying manners of the data trends emerged in **Figure 6**. As discussed previously, the different channel geometries between the furrowed[32] and pin-fin[33] channels have respectively led to the negative and positive ψ_2 values in

Figure 6. But the common feature of the reduced magnitudes of ψ_2 values caused by increasing *Ro* is observed for the two types of rotating channels[32,33] in **Figure 6**. Having correlated the ψ_2 values and the Nu/Nu_0 ratios at zero-buoyancy conditions into the *Ro* functions, the heat transfer correlations, which permit the evaluation of the isolated and coupled *Ro* and *Bu* effects on Nu/Nu_0, is generated for the particular rotating channel.

FIGURE LEGENDS:

Figure 1. Realistic operating *Re*, *Ro* and *Bu* ranges and the emulated laboratory conditions for a rotating coolant channel in a gas turbine rotor blade. The test conditions performed by NASA HOST program[3-6] are indicated as the bar symbol. The open and solid symbols respectively signify the *Bu*, *Ro*, and *Re* test ranges for the pointed and full-field heat transfer measurements. Numbers in brackets are references from which data are taken.

Figure 2. Typical heat loss coefficients (h_{loss}) at various rotating speeds[30] using the trapezoidal twin-pass rib-roughened rotating channel as an illustrative example. The diagram at the top depicts the constructional details of the rotating test module. The slope of each data trend constituted by the heat loss flux against the wall-to-ambient temperature difference shown in the left lower portion reveals the heat loss coefficient at the specific rotating speed. By correlating the heat loss coefficients detected at all the rotating speed tested, the generated heat loss correlation typified by the right lower plot is incorporated into the data processing program for *Nu* accountancy. The error bars in the lower right plot indicate the ranges of h_{loss}[30].

Figure 3. Local Nusselt number distribution of the static twin-pass S-channel roughened by curly ribs at *Re* = 15,000 measured by present infrared thermography method. The top diagram depicts the endwall of the two-pass wavy channel and the longitudinal S-ribs. As indicated by the AA' section view, the pair of longitudinal S-ribs is arranged inline on two opposite channel endwalls. In the detailed distribution of Nusselt number over the two-pass wavy endwall shown as the lower plot, the *Nu* data along the two longitudinal S-ribs are discarded due to the wall conduction effects on the distributions of heat-flux and wall-temperature.

Figure 4. Examples demonstrating the isolation of *Re* impact from *Ro* and *Bu* effect on local and regionally-averaged heat transfer properties of rotating channel. The upper portion exhibits the detailed Nusselt number distributions at a fixed *Ro* of 0.15 with a different *Re* of 5000, 7500, and 12,500 to enlighten the impacts of Reynolds number on the heat transfer properties of the rotating endwall. The lower portion depicted the area-averaged heat transfer properties over the rotational leading and trailing endwalls. The normalized Nu/Nu_0 ratios highlight the heat transfer variations from the non-rotating scenarios by rotation. Adapted with permission from Chang *et al.* 2017[31].

Figure 5. Examples demonstrating the uncoupled *Ro* effect from *Bu* impact on heat transfer properties of rotating channel[32,33]. Each *Bu*-driven Nu/Nu_0 variation is obtained at the fixed *Ro* and correlated as a linear function of *Bu* as indicated by the straight line in each plot. The correlation coefficients of these fitted lines fall between 0.96 and 0.98. The extrapolation of the Nu/Nu_0 data trend toward $Bu \rightarrow 0$ along each fitted line reveals the Nu/Nu_0 ratio at the tested *Ro*.

The magnitude and slope of each *Bu*-driven Nu/Nu_0 data trend disclose the manners of buoyancy effect on heat transfer performances. The magnitudes of the slopes represent the degrees of *Bu* impact on Nu/Nu_0. The positive and negative slopes respectively reflect the improving and impairing buoyancy impact on heat transfer levels. Numbers in brackets are references from which data are taken.

Figure 6. Uncoupled *Ro* and *Bu* effects on regionally averaged heat transfer performances of the rotating wavy channel[32,33]. The upper portion collects the heat transfer scenarios at various *Ro* but with vanished buoyancy effect at *Bu* = 0. Such Nu/Nu_0 variations are solely caused by the various Coriolis forces at different *Ro*. The lower portion shows the variations of *Bu* impact on Nu/Nu_0 at different *Ro*. The negative and positive ψ_2 values indicate the respective impairing and improving *Bu* impacts on the heat transfer performances for the furrowed[32] and pin-fin[33] channels. The dotted lines in this Figure are the correlation results for Nu/Nu_0 at *Bu* = 0. Numbers in brackets are references from which data are taken.

DISCUSSION:

While the endwall temperatures of a rotating channel are detected by an infrared thermography system, the fluid temperatures are measured by thermocouples. As the alternative magnetic field of an AC motor that drives a rotating rig induces electrical potential to interfere the thermocouple measurements, the DC motor must be adopted to drive a rotating test rig.

The fluid temperature distribution over the exit plane of a heated channel is not uniform. At least five thermocouples on the existing plane of a rotating channel are recommended for measuring the local fluid exit temperatures. In particular, these thermocouples measuring the fluid temperatures installed in the flow passage are subject to centrifugal forces during the rotating tests. The thermocouple wires are easily bent toward the hot channel walls. Thus, a shielded thermocouple cable for measuring the fluid entry temperature is used. On the flow exit plane, a mesh with several thermocouple beads weaved on the mesh can be sandwiched between the exit flanges of a test channel to detect the fluid exit temperatures at the predefined locations under a rotating test condition.

With considerable rotation induced buoyancy effects on the flow and heat transfer characteristics of a rotating channel, the method selected to detect the full-field heat transfer data needs to include both Coriolis-force and buoyancy effects. Using the transient liquid crystal method for measuring the full-field heat transfer data, the thermal boundary layers are not yet fully developed as the temporal channel-wall temperature variations are essential by this method for acquiring the convective heat transfer coefficients. As the centripetal acceleration could reach 10^5 x g in a coolant channel of a rotating gas turbine blade, the heat transfer data subject to the influences of the fully developed buoyancy flows, which are detectable by the present experimental method, are more practical for design activities.

The exposure of the scanned hot channel wall to an infrared camera inevitably incurs heat loss from the Joule heat generated by the heating foils. The protocols for conducting the heat loss calibration tests are critical for ensuring the quality of heat transfer data. Inheriting either from

the free or forced convective external flows for a static or rotating test channel, the convective heat transfer coefficients can be correlated as the function of wall-to-ambient temperature difference at a fixed rotating speed (**Figure 2**). It is preferable to envelop the entire rotating heat transfer test module with a shield for recovering the "free-convective" like external flows during the rotating tests. The maximum experimental uncertainties of heat transfer data are generally reduced when the percentage of the heat loss flux from the supplied heat flux is reduced. Nevertheless, the heat loss coefficients are slightly increased as *N* increases even with the enveloped shield covering the entire heat transfer test module (**Figure 3**). The heat loss correlation is included in the post data processing program to evaluate the distribution of local heat loss flux for each set of heat transfer test results. As the thermal inertia of the heat transfer module filled by thermal insulation material is considerably increased, the time required for reaching the steady-state condition during each heat loss test is considerably extended from a heat transfer test with airflow.

It is essential to investigate the applicability of the isolating *Re* effect on heat transfer properties from those induced by rotation. As the *Re* effect on heat transfer performances depends on the channel configurations, it is not appropriate to customarily adopt the heat transfer correlations generated from other channel geometries as the static-channel heat transfer references. The present experimental method isolates *Re* impact from *Ro* and *Bu* effects by presenting the heat transfer data in terms of Nu/Nu_0, in which the Nu_0 data are measured for the static test channel. While the buoyancy effect in a rotation channel with centripetal acceleration about 10^5 x g is considerable, the gravitation-driven buoyancy effect on the heat transfer property of a static channel is generally negligible within the typical range of fluid density ratios examined for a static test channel.

During a heat transfer test after feeding heater power to generate the required temperature gradients for facilitating heat convection, a certain degree of buoyancy effect driven by the induced centripetal acceleration field in the rotating channel is inevitable. Such coupled *Ro* and *Bu* effects for a rotating channel at the realistic engine conditions are not negligible due to the extremely high centripetal accelerations. Thus, both Coriolis force and rotating buoyancy level are simultaneously altered when the rotating speed is adjusted. The simultaneous control of *Ro* and *Re* at the targeting values during the rotating experiment is essential for decoupling the *Ro* and *Bu* effects on heat transfer properties. Having fixed both *Ro* and *Re*, the heat transfer variations corresponding to the variation of heat flux, or buoyancy level, reflect the rotating buoyancy effect on heat transfer properties at the tested *Ro*. The Nu/Nu_0 data converted from the data set generated in this manner permit the implementation of steps 7.4 - 7.8 for identifying the Coriolis force effect and rotating buoyance effect in isolation.

The *Bu* impact on the heat transfer property of a rotating channel is often *Ro* dependent as exemplified by **Figure 6** in which the ψ_2 values are varied as *Ro* changes. It is not appropriate to select the mathematic structure of the heat transfer correlation that treats the *Ro* and *Bu* as the independent parameters in the correlation.

In view of the Nu/Nu_0 extrapolation toward the limiting condition of $Bu \rightarrow 0$, the linear-like Nu/Nu_0

variations against the selected buoyancy parameter is preferable in order to reduce the uncertainty caused by the data extrapolation. In this regard, the fluid density ratio, $\Delta\rho/\rho$ or the buoyancy number, *Bu*, is recommended as the buoyancy parameter for disclosing the zero-buoyancy Nu/Nu_0 level during such data extrapolating process.

With high pressure rotating tests, the deformations of heating foils and the constituent components of a rotating channel due to the thermal expansions at various patterns of temperature distribution often cause airflow leakage during the rotating test. Such small airflow leakage is difficult to be identified during the rotating test. Thus, immediate subsequent data processing is recommended for acquiring the heat transfer data of the rotating channel. By cross-examining the heat transfer results obtained from the previous rotating tests, the implication of any inconsistent data trend is the possible airflow leakage. The subsequent measures to detect and then prevent the airflow leakage are required.

We have demonstrated a method for generating the heat transfer data of a rotating channel at the realistic engine conditions with the Coriolis-force effect and rotating buoyancy effect uncoupled. The major limitation of the present experimental method for extending the test ranges of *Ro* and *Bu* is the sustainability of the infrared camera that rotates with the test channel. In general, 10 x g is the maximum sustainable centrifugal acceleration for an infrared camera. With respect to the existing method detecting the heat transfer rates of a rotating channel, the use of thin heating foil can minimize the effects of channel-wall conduction on the distribution of local convective heat flux and the detection of temperatures at wall-fluid interfaces. Also, the two-dimensional full-field heat transfer distribution over a rotating surface subject to the steady-state buoyancy effect are detectable using the present experimental technique. With the data analysis method developed, the influences of Coriolis force and rotating buoyancy on the full-field heat transfer property of a rotating channel can be uncoupled. This method has already been applied to a wide range of rotating channel configurations. We expect that the present experimental strategy can lead to the design- friendly heat transfer correlations and which will continue to extend for the full coverage of realistic engine conditions when the advancement of infrared camera technology permits its usages at the conditions with higher centrifugal accelerations.

ACKNOWLEDGMENTS:

The present research work was financially sponsored by the Ministry of Science and Technology of Taiwan under the grant NSC 94-2611-E-022-001, NSC 95-2221-E-022-018, NSC 96-2221-E-022-015MY3 and NSC 97-2221-E-022-013-MY3.

DISCLOSURES:

The authors have nothing to disclose.

REFERENCES:

1. Morris, W.D. Heat transfer and fluid flow in rotating coolant channels. John Wiley and Sons, ISBN 0471101214 (1981).

2. Morris, W.D. A rotating facility to study heat transfer in the cooling passage of turbine rotor blades. *Journal of Power and Energy*. **210** (1), 55-63, 10.1243/PIME_PROC_1996_210_008_02 (1996).
3. Wagner, J.H., Johnson, B.V., Graziani, R.A., Yeh, F.C. Heat transfer in rotating passages with smooth walls and radially outward flow. *ASME Journal of Turbomachinery*. **113** (1), 42-51, 10.1115/1.2927736 (1991).
4. Wagner, J.H., Johnson, B.V., Kopper, F.C. Heat transfer in rotating serpentine passages with smooth walls. *ASME Journal of Turbomachinery*. **113** (3), 321-330, 10.1115/1.2927879 (1991).
5. Wagner, J.H., Johnson, B.V., Steuber, G.D., Yeh, F.C. Heat transfer in rotating serpentine passages with trips normal to the flow. *ASME Journal of Turbomachinery*. **114** (4), 847-857, 10.1115/1.2928038 (1992).
6. Johnson, B.V., Wagner, J.H., Steuber, G.D., Yeh, F.C. Heat transfer in rotating serpentine passages with selected model orientations for smooth or skewed trip walls. *ASME Journal of Turbomachinery*. **116** (4), 738-744, 10.1115/1.2929467 (1992).
7. Hwang, G.J., Tzeng, S.C., Mao, C.P., Soong, C. Y. Heat transfer in a radially rotating four-pass serpentine channel with staggered half-v rib turbulators. *ASME Journal of Heat Transfer*. **123** (1), 39-50, 10.1115/1.1338130 (2001).
8. Azad, G.S., Uddin, M.J., Han, J.C., Moon, H.K., Glezer, B. Heat transfer in a two-pass rectangular rotating channel with 45-deg angled rib turbulators. *ASME Journal of Turbomachinery*. **124** (2), 251-259, 10.1115/1.1450569 (2002).
9. Griffith, T.S., Al-Hadhrami, L., Han, J.C. Heat transfer in rotating rectangular cooling channels (AR=4) with angled ribs. *ASME Journal of Heat Transfer*. **124** (4), 617-625, 10.1115/1.1471525 (2002).
10. Al-Hadhrami, L., Griffith, T.S., Han, J.C. Heat transfer in two-pass rotating rectangular channels (AR=2) with five different orientations of 45 deg V-shaped rib turbulators. *ASME Journal of Heat Transfer*. **125** (2), 232-242, 10.1115/1.1561455 (2003).
11. Chang, S.W., Liou, T.M., Hung, J.H., Yeh, W.H. Heat transfer in a radially rotating square-sectioned duct with two opposite walls roughened by 45 deg staggered ribs at high rotation numbers. *ASME Journal of Heat Transfer*. **129** (2), 188-199, 10.1115/1.2409988 (2007).
12. Zhou, F., Lagrone, J., Acharya, S. Internal cooling in 4:1 AR passages at high rotation numbers. ASME Journal of Heat Transfer. **129** (12), 1666-1675, 10.1115/1.2767676 (2007).
13. Liu, Y.H., Huh, M., Han, J.C., Chopra, S. Heat transfer in a two-pass rectangular channel (AR=1:4) under high rotation numbers. *ASME Journal of Heat Transfer*. **130** (8), 081701-1-9, 10.1115/1.2909615 (2008).
14. Chang, S.W., Liou, T.M., Chiou, S.F., Chang, S.F. Heat transfer in high-speed rotating trapezoidal duct with rib-roughened surfaces and air bleeds from the wall on the apical side. *ASME Journal of Heat Transfer*. **130** (6), 061702-1-13, 10.1115/1.2891217 (2008).
15. Wright, L.M., Liu, Y.H., Han, J.C., Chopra, S. Heat transfer in trailing edge, wedge-shaped cooling channels under high rotation numbers. *ASME Journal of Heat Transfer*. **130** (7), 071701-1-11, 10.1115/1.2907437 (2008).
16. Liou, T.M., Chen, M.Y., Tsai, M.H. Fluid flow and heat transfer in a rotating two-pass square duct with in-line 90-deg ribs. *ASME Journal of Turbomachinery*. **124** (2), 260-268, 10.1115/1.1459079 (2002).
17. Chang, S.W., Liou, T.M., Yang, T.L., Hong, G.F. Heat transfer in radially rotating pin-fin channel

at high rotation numbers. *ASME Journal of Turbomachinery*. **132** (2), 021019-1-12, 10.1115/1.3147103 (2010).
18. Rallabandi, A., Lei, J., Han, J.C., Azad, S., Lee, C.P. Heat transfer measurements in rotating blade–shape serpentine coolant passage with ribbed walls at high Reynolds numbers. A*SME Journal of Turbomachiner*y. **136** (9), 091004-1-9, 10.1115/1.4026945 (2014).
19. Mayo, I., Arts, T., Ahmed, E.H., Parres, B. Two-dimensional heat transfer distribution of a rotating ribbed channel at different Reynolds numbers. *ASME Journal of Turbomachinery*. **137** (3), 031002-1-11, 10.1115/1.4028458 (2015).
20. Chang, S.W., Yang, T.L., Liou, T.M., Fang, H.G. Heat transfer in rotating scale-roughened trapezoidal duct at high rotation numbers. *Applied Thermal Engineering*. **29** (8), 1682-1693, 10.1016/j.applthermaleng.2008.07.024 (2009).
21. Liou, T. M., Chang, S.W., Chen, J.S., Yang, T.L., Lan, Y.A. Influence of channel aspect ratio on heat transfer in rotating rectangular ducts with skewed ribs at high rotation numbers. *International Journal of Heat Mass Transfer.* **52** (23), 5309-5322, 10.1016/j.ijheatmasstransfer.2009.07.013 (2009).
22. Huh, M., Liu, Y.H., Han, J.C. Effect of rib height on heat transfer in a two pass rectangular channel (AR = 1:4) with a sharp entrance at high rotation numbers. *International Journal of Heat Mass Transfer.* **52** (19), 4635-4649, 10.1016/j.ijheatmasstransfer.2009.07.013 (2009).
23. Xu, G., Li, Y., Deng, H. Effect of rib spacing on heat transfer and friction in a rotating two-pass square channel with asymmetrical 90-deg rib turbulators. *Applied Thermal Engineering*. **80** (5), 386-395, 10.1016/j.applthermaleng.2015.02.011 (2015).
24. Tao, Z., Yang, M., Deng, H., Li, H., Tian, S. Heat transfer study in a rotating ribbed two-pass channel with engine-similar cross section at high rotation number. *Applied Thermal Engineering.* **106** (5), 681-696, 10.1016/j.applthermaleng.2016.06.053 (2016).
25. Li, Y., Deng, H., Tao, Z., Xu, G., Chen, Y. Heat transfer characteristics in a rotating trailing edge internal cooling channel with two coolant inlets. *International Journal of Heat Mass Transfer.* **105** (2), 220-229, 10.1016/j.ijheatmasstransfer.2016.08.114 (2017).
26. Deng, H., Chen, Y., Tao, Z., Li, Y., Qiu, L. Heat transfer in a two-inlet rotating rectangular channel with side-wall fluid extraction. *International Journal of Heat and Mass Transfer*. **105** (2), 525-534, 10.1016/j.ijheatmasstransfer.2016.10.027 (2017).
27. You, R., Li, H., Tao, Z., Wei, K. Heat transfer investigation in a smooth rotating channel with thermography liquid crystal. ASME Turbo Expo. GT2016-56413, *Turbomachinery Technical Conference and Exposition: Heat Transfer*. **5** (B), V05BT16A006 1~10, 201610.1115/GT2016-56413 (2016).
28. Morris, W.D., Chang, S.W. An experimental study of heat transfer in a simulated turbine blade cooling passage. *International Journal of Heat Mass Transfer*. **40** (15), 3703-3716, 10.1016/S0017-9310(96)00311-0 (1997).
29. Chang, S.W., Liou, T.-M., Po. Y. Coriolis and rotating buoyancy effect on detailed heat transfer distributions in a two-pass square channel roughened by 45° ribs at high rotation numbers. *International Journal of Heat Mass Transfer*. **53** (7), 1349-1363, 10.1016/j.ijheatmasstransfer. 2009.12.024 (2010).
30. Wang, W.J. Heat transfer in rotating twin-pass trapezoidal-sectioned passage with two opposite walls roughened by 45 degree ribs. Msc thesis, Department of Marine Engineering, National Kaohsiung Marine University, (2006).

31. Chang, S.W., Wu, P.-S., Chen, C.-S., Weng, C.-C., Jiang, Y.-R., Shih, S.-H. Thermal performance of radially rotating two-pass S-shaped zig-zag channel. *International Journal of Heat and Mass Transfer*. **115** (B), 1011-1031, 10.1016/j.ijheatmasstransfer.2017.08.111 (2017).
32. Chang, S.W., Lees, A. W., Liou, T.-M., Hong, G.F. Heat transfer of a radially rotating furrowed channel with two opposite skewed sinusoidal wavy walls. *International Journal of Thermal Sciences.* **49** (5), 769-785, 10.1016/j.ijthermalsci.2009.11.011 (2010).
33. Chang, S.W., Liou, T.-M., Lee, T.-H, Heat transfer of a rotating rectangular channel with a diamond-shaped pin-fin array at high rotation numbers. *Journal of Turbomachinery Transactions of the ASME*. **135** (4), 041007 1~10, 10.1115/1.4007684 (2013).
34. Morris, W.D., Chang, S.W., Heat transfer in a radially rotating smooth-walled tube, *The Aeronautical Journal*. **102** (1015), 277-285, 10.1017/S0001924000065313 (1998).

Figure

Click here to download Figure Figure 1.tif

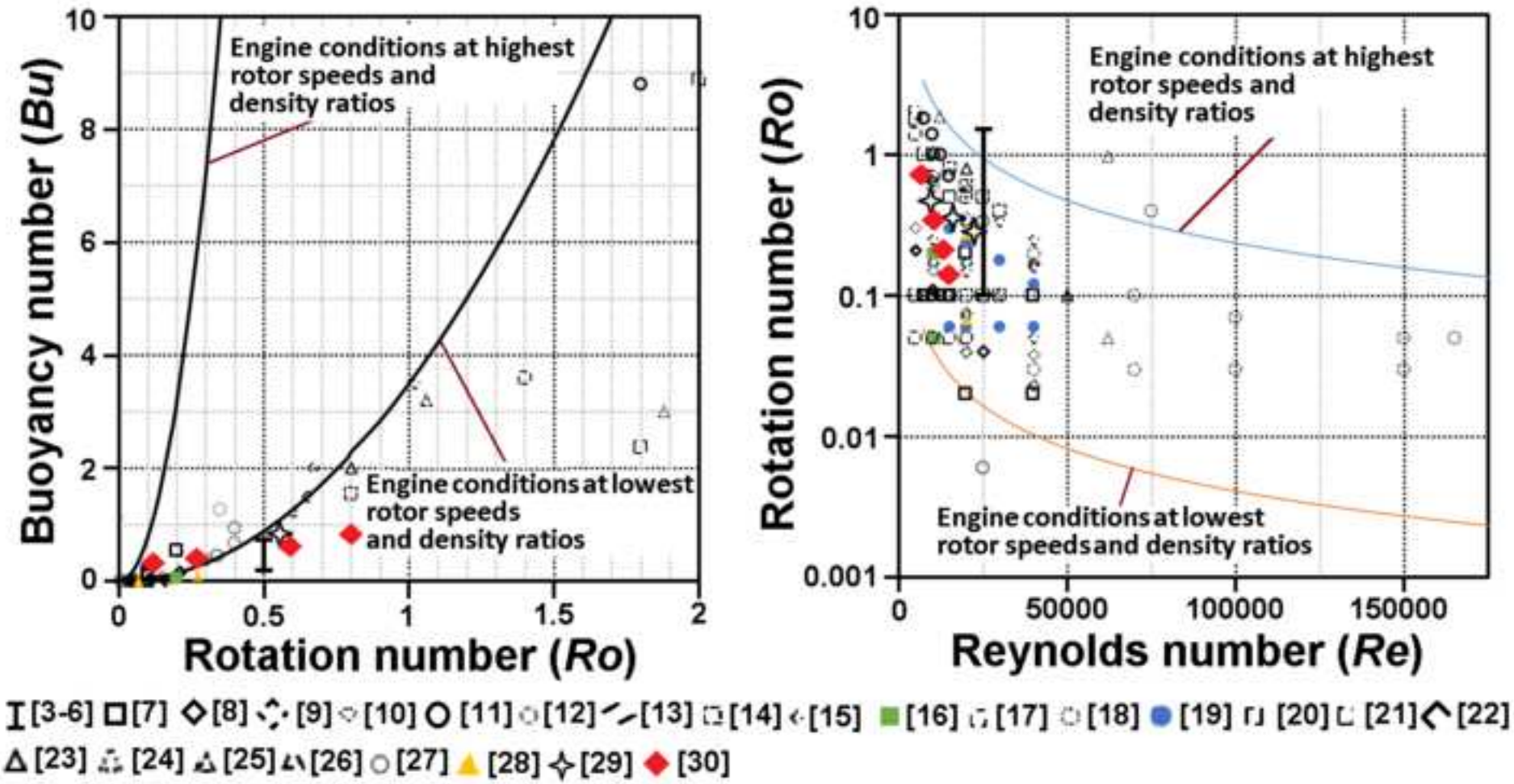

Figure

Click here to download Figure Figure 2.tif

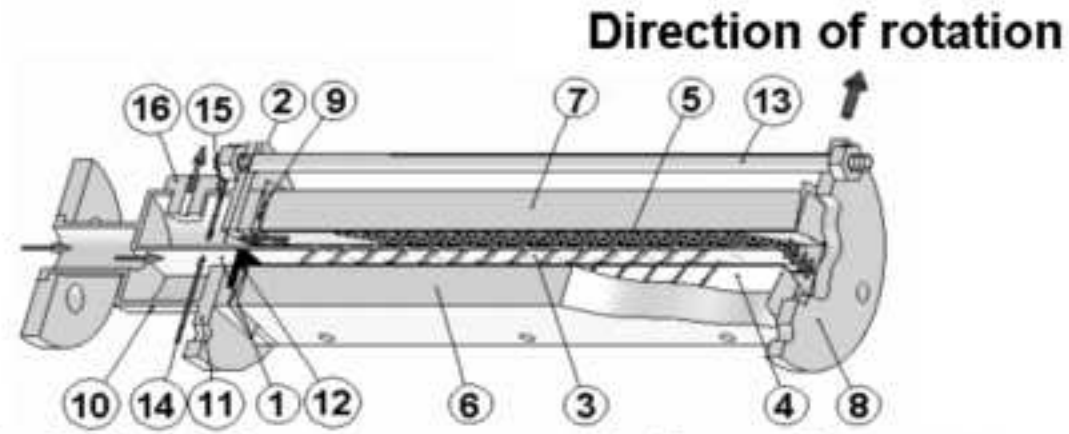

(1) Radial outward flow passage
(2) Radially inward flow passage
(3) Two sides rib-roughened divider
(4)(5) Rib-roughened stainless-steel heating foils
(6)(7) Tufnol sidewalls
(8) Top Tufnol flange
(9) Bottom copper plates
(10) Cylindrical plenum chamber
(11) Bottom end flange
(12) Mesh layers
(13) Draw bolts
(14) Thermocouple measuring flow entry temperature
(15) Thermocouples measuring flow exit temperature
(16) Exit tapping plug

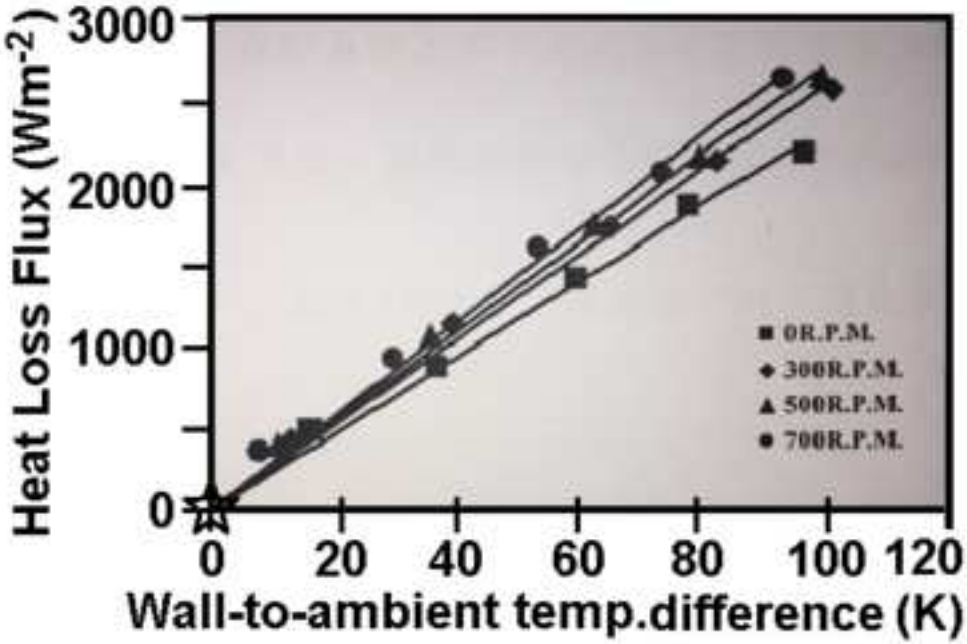

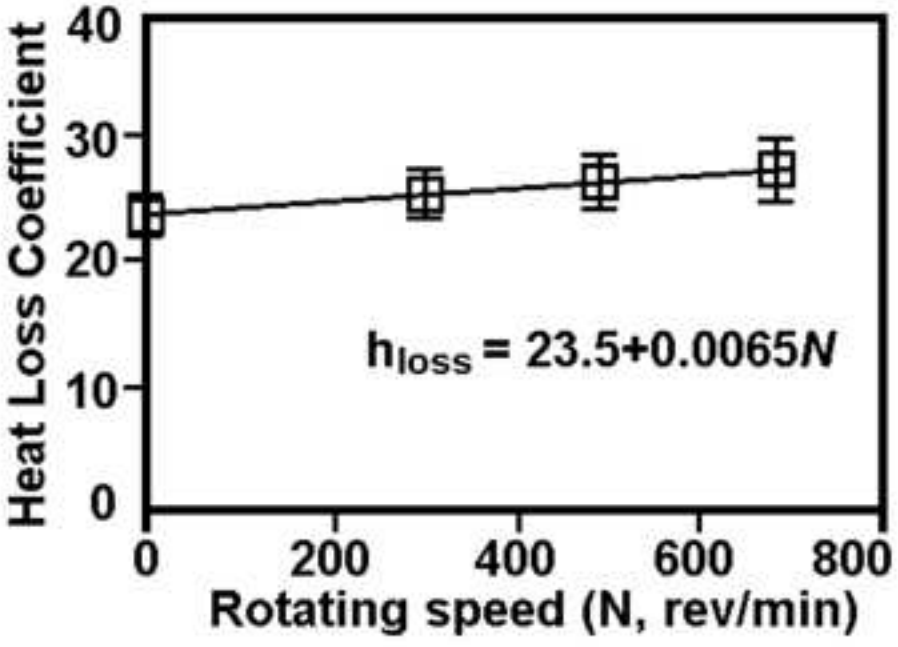

Figure

Click here to download Figure Figure 3.tif

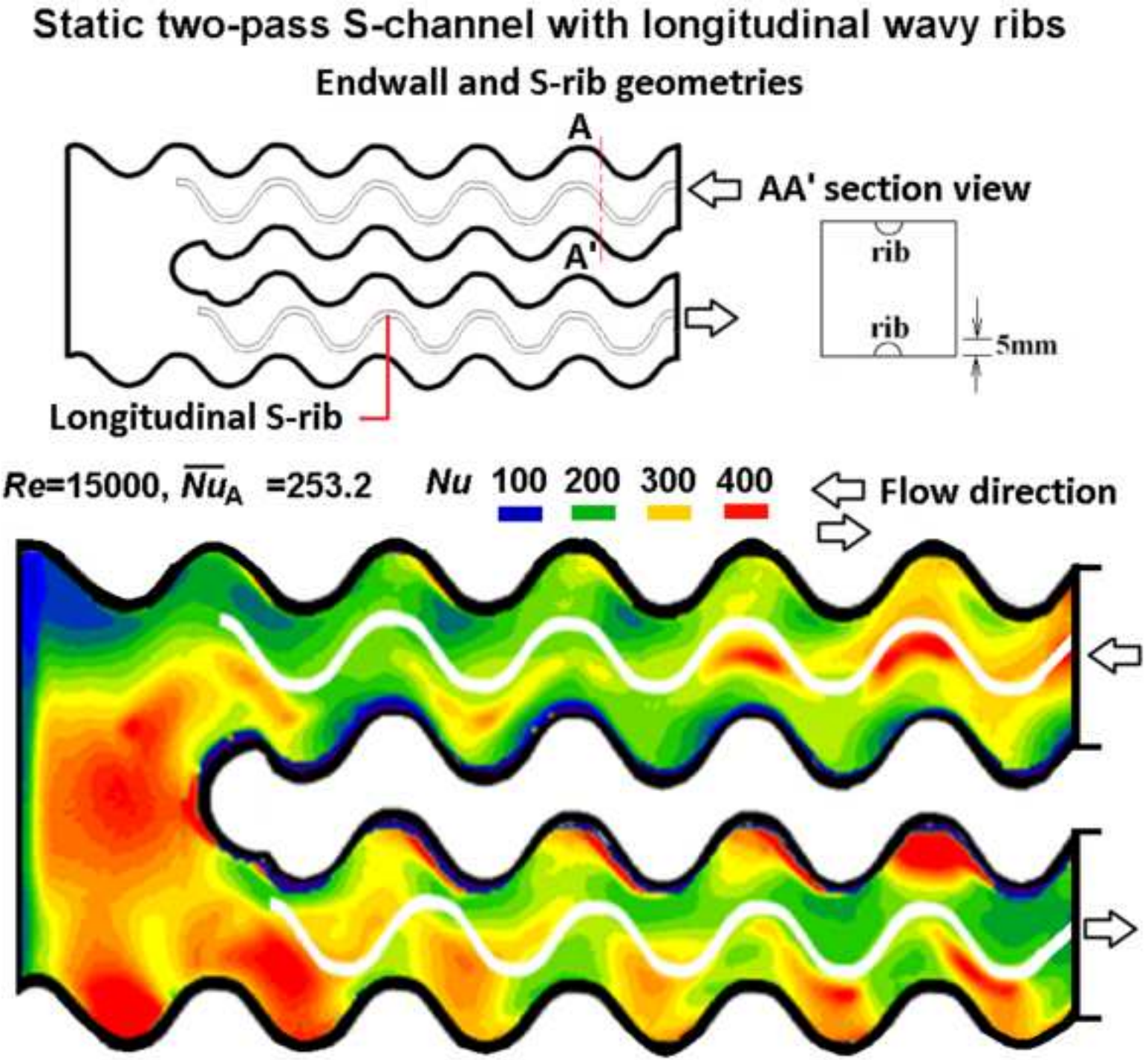

Figure

Click here to download Figure Figure 4.tif

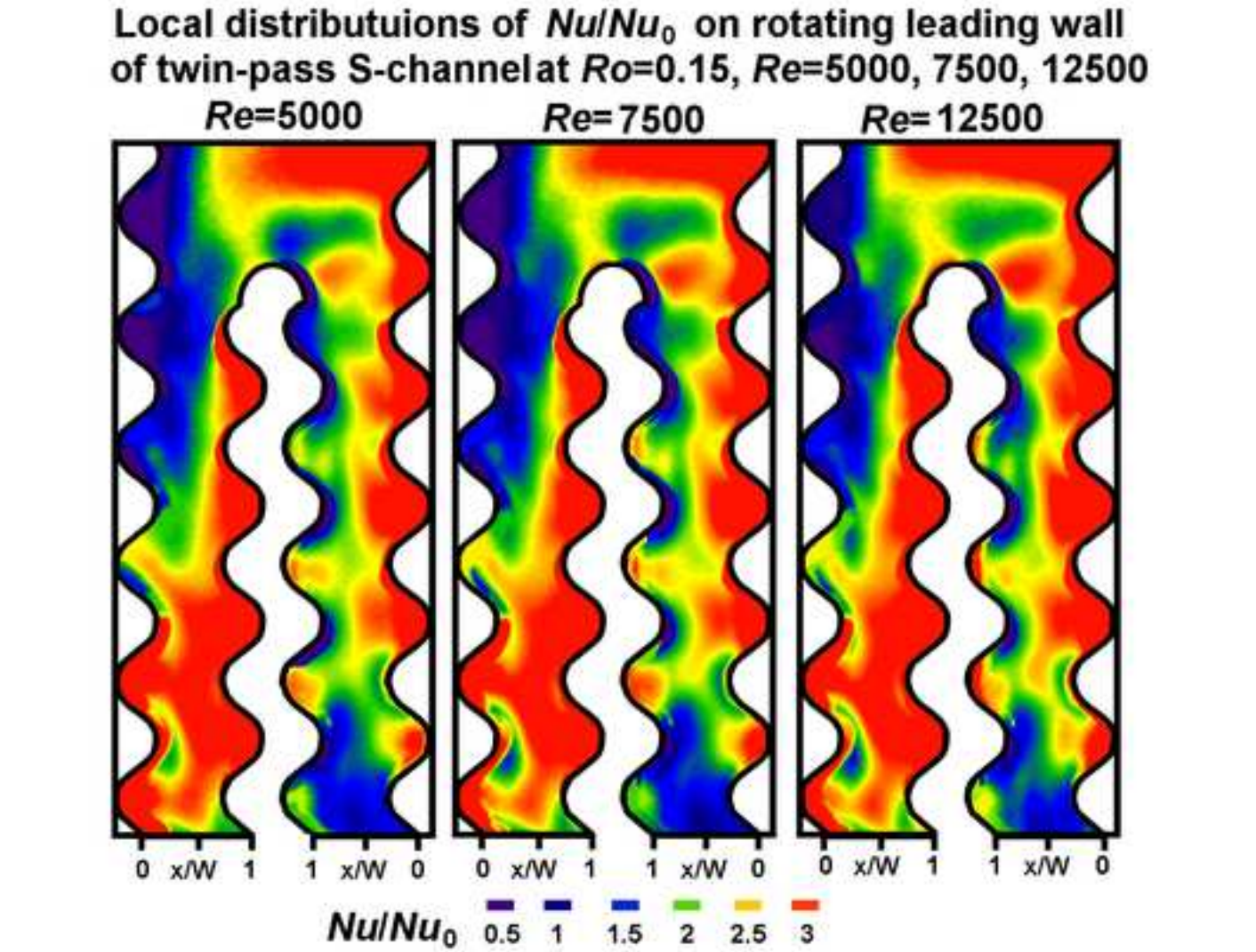

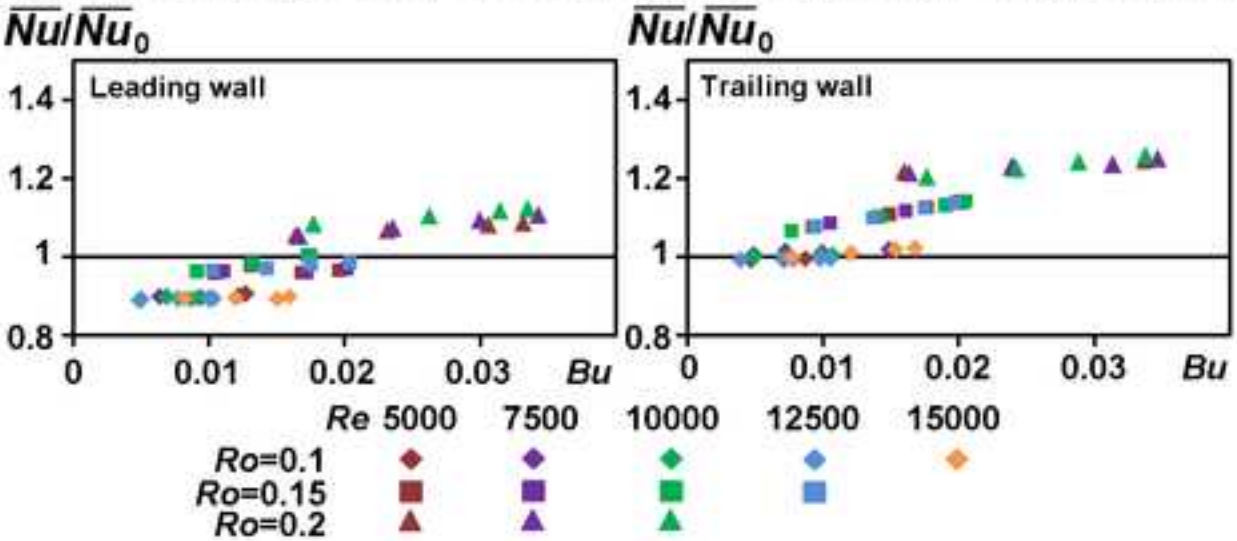

Figure

Click here to download Figure Figure 5.tif

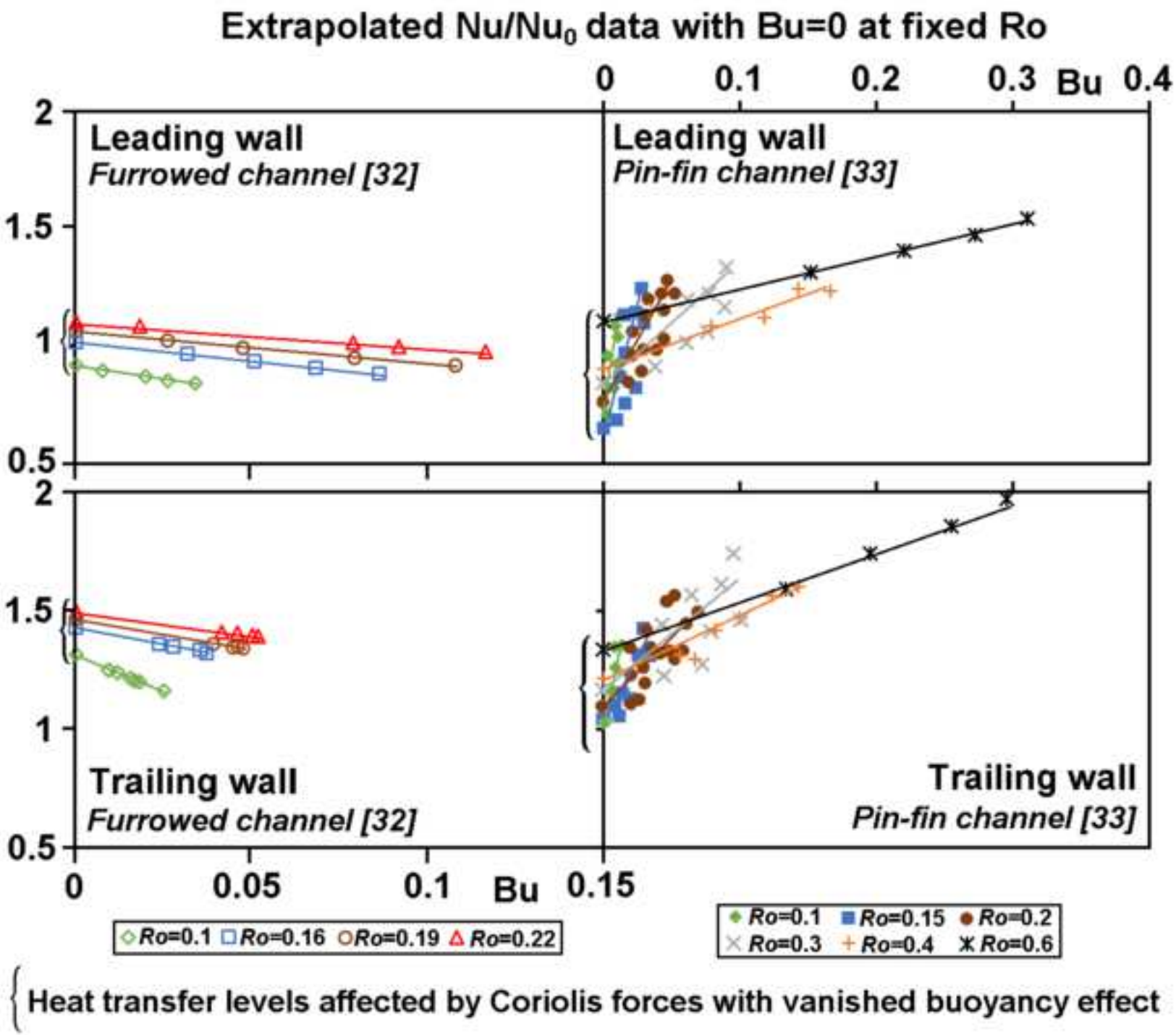

Figure

Click here to download Figure Figure 6.tif

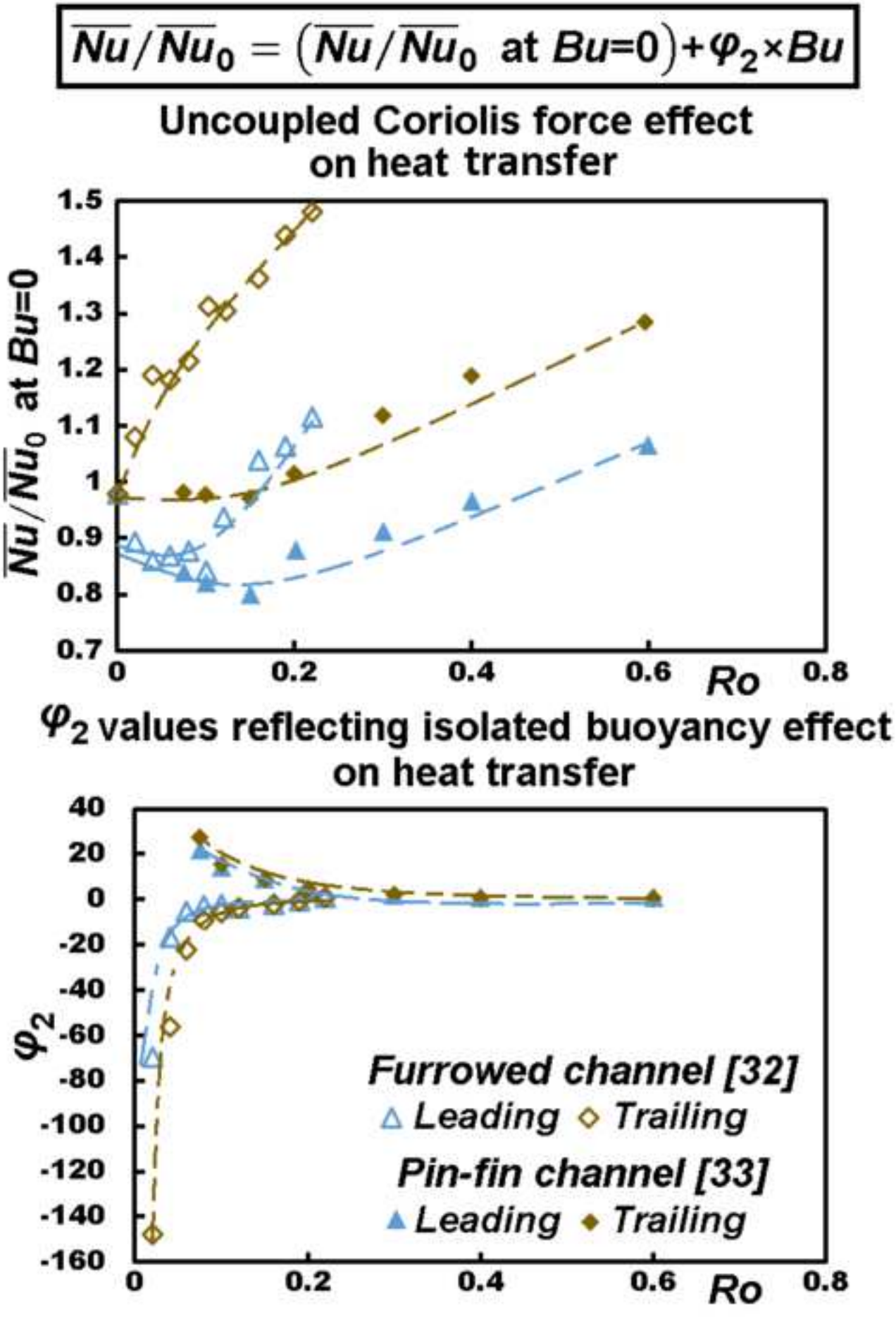

Materials Table

Click here to download Materials Table JoVE_Materials.xls

Name of Material/ Equipment	Company	Catalog Number	Comments/Description
Name of Material/Equipment	Company	Catalog Number	Comments/Description
Rotating test rig	In-house made		Design by this research group
Heat transfer test module	In-house made		Design by this research group
Mass flow meter	Eldride Product, Inc.	3100301-01-01 359-1007	
Infrared thermography system	NEC P384A-8	3100401-04 3127A-4	
Instrumentation slip ring	Michigan Scientific SR36M	3100506-62 3553-372	

jove JOURNAL OF VISUALIZED EXPERIMENTS
1 Alewife Center #200
Cambridge, MA 02140
tel. 617.945.9051
www.jove.com

ARTICLE AND VIDEO LICENSE AGREEMENT

Title of Article: An experimental method to unravel effects of Coriolis force and rotating buoyancy on full-field heat transfer property of a rotating channel

Author(s): Shyy Woei Chang, Hong-Da Shen, Kuo-Ching Yu

Item 1 (check one box): The Author elects to have the Materials be made available (as described at http://www.jove.com/author) via: ☑ Standard Access ☐ Open Access

Item 2 (check one box):

☑ The Author is NOT a United States government employee.

☐ The Author is a United States government employee and the Materials were prepared in the course of his or her duties as a United States government employee.

☐ The Author is a United States government employee but the Materials were NOT prepared in the course of his or her duties as a United States government employee.

ARTICLE AND VIDEO LICENSE AGREEMENT

1. Defined Terms. As used in this Article and Video License Agreement, the following terms shall have the following meanings: "**Agreement**" means this Article and Video License Agreement; "**Article**" means the article specified on the last page of this Agreement, including any associated materials such as texts, figures, tables, artwork, abstracts, or summaries contained therein; "**Author**" means the author who is a signatory to this Agreement; "**Collective Work**" means a work, such as a periodical issue, anthology or encyclopedia, in which the Materials in their entirety in unmodified form, along with a number of other contributions, constituting separate and independent works in themselves, are assembled into a collective whole; "**CRC License**" means the Creative Commons Attribution-Non Commercial-No Derivs 3.0 Unported Agreement, the terms and conditions of which can be found at: http://creativecommons.org/licenses/by-nc-nd/3.0/legalcode; "**Derivative Work**" means a work based upon the Materials or upon the Materials and other pre-existing works, such as a translation, musical arrangement, dramatization, fictionalization, motion picture version, sound recording, art reproduction, abridgment, condensation, or any other form in which the Materials may be recast, transformed, or adapted; "**Institution**" means the institution, listed on the last page of this Agreement, by which the Author was employed at the time of the creation of the Materials; "**JoVE**" means MyJove Corporation, a Massachusetts corporation and the publisher of *The Journal of Visualized Experiments;* "**Materials**" means the Article and / or the Video; "**Parties**" means the Author and JoVE; "**Video**" means any video(s) made by the Author, alone or in conjunction with any other parties, or by JoVE or its affiliates or agents, individually or in collaboration with the Author or any other parties, incorporating all or any portion of the Article, and in which the Author may or may not appear.

2. Background. The Author, who is the author of the Article, in order to ensure the dissemination and protection of the Article, desires to have the JoVE publish the Article and create and transmit videos based on the Article. In furtherance of such goals, the Parties desire to memorialize in this Agreement the respective rights of each Party in and to the Article and the Video.

3. Grant of Rights in Article. In consideration of JoVE agreeing to publish the Article, the Author hereby grants to JoVE, subject to **Sections 4** and **7** below, the exclusive, royalty-free, perpetual (for the full term of copyright in the Article, including any extensions thereto) license (a) to publish, reproduce, distribute, display and store the Article in all forms, formats and media whether now known or hereafter developed (including without limitation in print, digital and electronic form) throughout the world, (b) to translate the Article into other languages, create adaptations, summaries or extracts of the Article or other Derivative Works (including, without limitation, the Video) or Collective Works based on all or any portion of the Article and exercise all of the rights set forth in (a) above in such translations, adaptations, summaries, extracts, Derivative Works or Collective Works and (c) to license others to do any or all of the above. The foregoing rights may be exercised in all media and formats, whether now known or hereafter devised, and include the right to make such modifications as are technically necessary to exercise the rights in other media and formats. If the "Open Access" box has been checked in **Item 1** above, JoVE and the Author hereby grant to the public all such rights in the Article as provided in, but subject to all limitations and requirements set forth in, the CRC License.

1 Alewife Center #200
Cambridge, MA 02140
tel. 617.945.9051
www.jove.com

4. Retention of Rights in Article. Notwithstanding the exclusive license granted to JoVE in **Section 3** above, the Author shall, with respect to the Article, retain the non-exclusive right to use all or part of the Article for the non-commercial purpose of giving lectures, presentations or teaching classes, and to post a copy of the Article on the Institution's website or the Author's personal website, in each case provided that a link to the Article on the JoVE website is provided and notice of JoVE's copyright in the Article is included. All non-copyright intellectual property rights in and to the Article, such as patent rights, shall remain with the Author.

5. Grant of Rights in Video – Standard Access. This **Section 5** applies if the "Standard Access" box has been checked in **Item 1** above or if no box has been checked in **Item 1** above. In consideration of JoVE agreeing to produce, display or otherwise assist with the Video, the Author hereby acknowledges and agrees that, Subject to **Section 7** below, JoVE is and shall be the sole and exclusive owner of all rights of any nature, including, without limitation, all copyrights, in and to the Video. To the extent that, by law, the Author is deemed, now or at any time in the future, to have any rights of any nature in or to the Video, the Author hereby disclaims all such rights and transfers all such rights to JoVE.

6. Grant of Rights in Video – Open Access. This **Section 6** applies only if the "Open Access" box has been checked in **Item 1** above. In consideration of JoVE agreeing to produce, display or otherwise assist with the Video, the Author hereby grants to JoVE, subject to **Section 7** below, the exclusive, royalty-free, perpetual (for the full term of copyright in the Article, including any extensions thereto) license (a) to publish, reproduce, distribute, display and store the Video in all forms, formats and media whether now known or hereafter developed (including without limitation in print, digital and electronic form) throughout the world, (b) to translate the Video into other languages, create adaptations, summaries or extracts of the Video or other Derivative Works or Collective Works based on all or any portion of the Video and exercise all of the rights set forth in (a) above in such translations, adaptations, summaries, extracts, Derivative Works or Collective Works and (c) to license others to do any or all of the above. The foregoing rights may be exercised in all media and formats, whether now known or hereafter devised, and include the right to make such modifications as are technically necessary to exercise the rights in other media and formats. For any Video to which this Section 6 is applicable, JoVE and the Author hereby grant to the public all such rights in the Video as provided in, but subject to all limitations and requirements set forth in, the CRC License.

7. Government Employees. If the Author is a United States government employee and the Article was prepared in the course of his or her duties as a United States government employee, as indicated in **Item 2** above, and any of the licenses or grants granted by the Author hereunder exceed the scope of the 17 U.S.C. 403, then the rights granted hereunder shall be limited to the maximum rights permitted under such statute. In such case, all provisions contained herein that are not in conflict with such statute shall remain in full force and effect, and all provisions contained herein that do so conflict shall be deemed to be amended so as to provide to JoVE the maximum rights permissible within such statute.

8. Likeness, Privacy, Personality. The Author hereby grants JoVE the right to use the Author's name, voice, likeness, picture, photograph, image, biography and performance in any way, commercial or otherwise, in connection with the Materials and the sale, promotion and distribution thereof. The Author hereby waives any and all rights he or she may have, relating to his or her appearance in the Video or otherwise relating to the Materials, under all applicable privacy, likeness, personality or similar laws.

9. Author Warranties. The Author represents and warrants that the Article is original, that it has not been published, that the copyright interest is owned by the Author (or, if more than one author is listed at the beginning of this Agreement, by such authors collectively) and has not been assigned, licensed, or otherwise transferred to any other party. The Author represents and warrants that the author(s) listed at the top of this Agreement are the only authors of the Materials. If more than one author is listed at the top of this Agreement and if any such author has not entered into a separate Article and Video License Agreement with JoVE relating to the Materials, the Author represents and warrants that the Author has been authorized by each of the other such authors to execute this Agreement on his or her behalf and to bind him or her with respect to the terms of this Agreement as if each of them had been a party hereto as an Author. The Author warrants that the use, reproduction, distribution, public or private performance or display, and/or modification of all or any portion of the Materials does not and will not violate, infringe and/or misappropriate the patent, trademark, intellectual property or other rights of any third party. The Author represents and warrants that it has and will continue to comply with all government, institutional and other regulations, including, without limitation all institutional, laboratory, hospital, ethical, human and animal treatment, privacy, and all other rules, regulations, laws, procedures or guidelines, applicable to the Materials, and that all research involving human and animal subjects has been approved by the Author's relevant institutional review board.

10. JoVE Discretion. If the Author requests the assistance of JoVE in producing the Video in the Author's facility, the Author shall ensure that the presence of JoVE employees, agents or independent contractors is in accordance with the relevant regulations of the Author's institution. If more than one author is listed at the beginning of this Agreement, JoVE may, in its sole discretion, elect not take any action with respect to the Article until such time as it has received complete, executed Article and Video License Agreements from each such author. JoVE reserves the right, in its absolute and sole discretion and without giving any reason therefore, to accept or decline any work submitted to JoVE. JoVE and its employees, agents and independent contractors shall have

jove JOURNAL OF VISUALIZED EXPERIMENTS
1 Alewife Center #200
Cambridge, MA 02140
tel. 617.945.9051
www.jove.com

ARTICLE AND VIDEO LICENSE AGREEMENT

full, unfettered access to the facilities of the Author or of the Author's institution as necessary to make the Video, whether actually published or not. JoVE has sole discretion as to the method of making and publishing the Materials, including, without limitation, to all decisions regarding editing, lighting, filming, timing of publication, if any, length, quality, content and the like.

11. Indemnification. The Author agrees to indemnify JoVE and/or its successors and assigns from and against any and all claims, costs, and expenses, including attorney's fees, arising out of any breach of any warranty or other representations contained herein. The Author further agrees to indemnify and hold harmless JoVE from and against any and all claims, costs, and expenses, including attorney's fees, resulting from the breach by the Author of any representation or warranty contained herein or from allegations or instances of violation of intellectual property rights, damage to the Author's or the Author's institution's facilities, fraud, libel, defamation, research, equipment, experiments, property damage, personal injury, violations of institutional, laboratory, hospital, ethical, human and animal treatment, privacy or other rules, regulations, laws, procedures or guidelines, liabilities and other losses or damages related in any way to the submission of work to JoVE, making of videos by JoVE, or publication in *JoVE* or elsewhere by JoVE. The Author shall be responsible for, and shall hold JoVE harmless from, damages caused by lack of sterilization, lack of cleanliness or by contamination due to the making of a video by JoVE its employees, agents or independent contractors. All sterilization, cleanliness or decontamination procedures shall be solely the responsibility of the Author and shall be undertaken at the Author's expense. All indemnifications provided herein shall include JoVE's attorney's fees and costs related to said losses or damages. Such indemnification and holding harmless shall include such losses or damages incurred by, or in connection with, acts or omissions of JoVE, its employees, agents or independent contractors.

12. Fees. To cover the cost incurred for publication, JoVE must receive payment before production and publication the Materials. Payment is due in 21 days of invoice. Should the Materials not be published due to an editorial or production decision, these funds will be returned to the Author. Withdrawal by the Author of any submitted Materials after final peer review approval will result in a US$1,200 fee to cover pre-production expenses incurred by JoVE. If payment is not received by the completion of filming, production and publication of the Materials will be suspended until payment is received.

13. Transfer, Governing Law. This Agreement may be assigned by JoVE and shall inure to the benefits of any of JoVE's successors and assignees. This Agreement shall be governed and construed by the internal laws of the Commonwealth of Massachusetts without giving effect to any conflict of law provision thereunder. This Agreement may be executed in counterparts, each of which shall be deemed an original, but all of which together shall be deemed to me one and the same agreement. A signed copy of this Agreement delivered by facsimile, e-mail or other means of electronic transmission shall be deemed to have the same legal effect as delivery of an original signed copy of this Agreement.

A signed copy of this document must be sent with all new submissions. Only one Agreement required per submission.

CORRESPONDING AUTHOR:

Name: Shyy Woei Chang

Department: System and Naval Mechatronic Engineering

Institution: National Cheng Kung University

Article Title: An experimental method to uncouple effects of Coriolis and rotating buoyancy on full-field heat transfer property of a rotating channel

Signature: Shyy Woei Chang Date: 22/11/2017

Please submit a signed and dated copy of this license by one of the following three methods:

1) Upload a scanned copy of the document as a pfd on the JoVE submission site;
2) Fax the document to +1.866.381.2236;
3) Mail the document to JoVE / Attn: JoVE Editorial / 1 Alewife Center #200 / Cambridge, MA 02139

For questions, please email submissions@jove.com or call +1.617.945.9051

Review comments for JoVE57630R2

We sincerely appreciated for the kind efforts and time for providing the following editorial comments aimed at improving the quality of the manuscript. We have fully responded all the Editorial comments. In the revised manuscript, the modifications and corrections for English usages are indicated as the red bars at the No. of sentences. The modifications and corrections made to respond the rest of comments are indicated as the pink prints in the revised manuscript. In what follows, the itemized responses are summarized.

Editorial comments:

1. **There are still numerous grammar and usage errors; please proofread, ideally by a fluent English speaker.**

I have ask the helps from my friend Andrew Neeson, Austrian native English speaker, to improve the English. All the modifications and corrections in the respect are indicated as the red prints in the revised manuscript.

2. **There are still a few inline variables made in an equation editor (e.g., in the paragraph after equation 1); please try to make these into Calibri text (note that this is not necessary, though, and may be impossible for some).**

To make this request possible, we have changed the vector symbols in the flow equations. Then all these inline variables are changed into Calibri texts.

3. Results: Ref. 32 is cited twice in one citation (Line 428).

The repeated citations for Ref. 32 is corrected. Thank you.

Protocol:

1. **Some of the protocol still seems to be lacking in detail (see below); detailed descriptions of how exactly the protocol is done (that is, what exactly someone who is carrying out the protocol should be doing) are necessary for planning of filming. Previous JoVE videos and their accompanying protocol text may help you get a better idea, in particular in the engineering section: https://www.jove.com/journal/engineering. Note that it is not necessarily a problem that construction of the module is not detailed, but operation of it should be explained more.**

The lacking details itemized in the following comments 2-7 are modified to enhance the descriptions of how exactly these protocols are done. Thank you for the helps.

2. 1.1: This is unclear, do you mean to simply choose a range of Re, Ro, and Bu?

The ranges of Re, Ro and Bu are determined in accordance with the operating conditions of a gas turbine rotor blade. Thus, protocol 1.1 is revised as:

1.1. Formulate the experimental conditions in terms of Re, Ro and Bu from the targeted operation conditions of a gas turbine rotor blade.

3. **1.4: Please include a citation here for design and construction.**

Reference 2 is cited for protocol 1.4. Thank you.

4. **2.4: How are temperatures read out? A display on the instrument? Computer display?**

The temperatures are read out on the computer screen. Protocol 2.4 is revised as below:

2.4. Feed electrical heating power through the heating foil and measure temperatures simultaneously by thermocouple and infrared thermography system from the computer display at the steady state.

5. **3.2: What is the vibrational limitation? How are conditions checked?**

The vibrational limitation is checked by viewing the instant temperature images displayed on the computer screen. The stable image allowing for data acquisition and transmission is needed. Protocol 3.2 is modified as below:

3.2. Adjust the counterbalancing weight gradually until the running condition of the rotating rig satisfies the vibrational limitation for the infrared thermographic measurements to exhibit the stable thermal image on the computer display.

6. **4.2: How is the module installed?**

Protocol 4.2 is revised into:

4.2. Install the filled test module on the rotating test rig by fitting the test module on the rotating platform and connecting the heater power supply and all the instrumental cables.

7. 5.1: How are heat transfer tests performed? It is unclear if this has been described in the previous steps.

The heat transfer tests are performed by feeding coolant flows and heater powers to the test module with all the relevant data monitored by the on-line data acquisition program. Protocol 5.1 is revised as below:

5.1 Perform heat transfer tests at the targeting Reynolds numbers at zero rotating speed (Ro=N=0) by feeding coolant flows and heater powers to the test module. Ensure the supplied coolant mass flow rate is constantly adjusted in order to control Reynolds number at the flow entry plane at the targeting value.

Figures:

1. **Please include more relevant details (e.g., what the error bars are and in general everything discussed below) in the Figure legends, instead of in the Results or Introduction, so that they can be more readily interpreted just from the legends.**

FIGURE LEGENDS:

Figure 1. Realistic operating Re, Ro and Bu ranges and the emulated laboratory conditions for a rotating coolant channel in a gas turbine rotor blade. The test conditions performed by NASA HOST program[3-6] are indicated as the bar symbol. The open and solid symbols respectively signify the Bu, Bo and Re test ranges for the pointed and full-field heat transfer measurements.

Figure 2. Typical heat loss coefficients (h_{loss}) at various rotating speeds[30] using the trapezoidal twin-pass rib-roughened rotating channel as an illustrative example. The

top portion depicts the constructional details of the rotating test module. The slope of each data trend constituting by the heat loss flux against wall-to-ambient temperature difference shown in the left lower portion reveals the heat loss coefficient at the specific rotating speed. By correlating the heat loss coefficients detected at all the rotating speed tested, the generated heat loss correlation typified by the right lower plot is incorporated into the data processing program for Nu accountancy.

Figure 3. Local Nusselt number distribution of the static twin-pass S-channel roughened by curly ribs at Re=15000 measured by present infrared thermography method. The top diagram depicts the endwall of two-pass wavy channel and the longitudinal S-ribs. As indicated by the AA' section view, the pair of longitudinal S-ribs is in-lined arranged on two opposite channel endwalls. In the detailed distribution of Nusselt number over the two-pass wavy endwall shown as the lower plot, the Nu data along the two longitudinal S-ribs are discarded due to the wall conduction effects on the distributions of heat-flux and wall-temperature.

Figure 4. Examples demonstrating the isolation of Re impact from Ro and Bu effect on local[31] and regionally-averaged heat transfer properties of rotating channel [31]. The upper portion exhibits the detailed Nusselt number distributions at fixed Ro of 0.15 with different Re of 5000, 7500 and 12500 to enlighten the impacts of Reynolds number on the heat transfer properties of the rotating endwall. The lower portion depicted the area-averaged heat transfer properties over the rotational leading and trailing endwalls. The normalized Nu/Nu_0 ratios highlight the heat transfer variations from the non-rotating scenarios by rotation.

Figure 5. Examples demonstrating the uncoupled Ro effect from Bu impact on heat transfer properties of rotating channel[32,33]. Each Bu-driven Nu/Nu_0 variation is obtained at the fixed Ro and correlated as a linear function of Bu as indicated by the straight line in each plot. The correlation coefficients of these fitted lines fall between 0.96 and 1.02. The extrapolation of the Nu/Nu_0 data trend toward $Bu \rightarrow 0$ along each fitted line reveals the Nu/Nu_0 ratio at the tested Ro. The magnitude and slope of each Bu-driven Nu/Nu_0 data trend disclose the manners of buoyancy effect on heat transfer performances. The magnitudes of the slopes represent the degrees of Bu impact on Nu/Nu_0. The positive and negative slopes respectively reflect the improving and impairing buoyancy impact on heat transfer levels.

Figure 6. Uncoupled Ro and Bu effects on regionally averaged heat transfer performances of the rotating wavy channel[32,33]. The upper portion collects the heat transfer scenarios at various Ro but with vanished buoyancy effect at Bu=0. Such Nu/Nu_0 variations are solely caused by the various Coriolis forces at different Ro. The lower portion shows the variations of Bu impact on Nu/Nu_0 at different Ro. The negative and positive ψ_2 values indicate the respective impairing and improving Bu impacts on the heat transfer performances for the furrowed[32] and pin-fin[33] channels.

2. **Figure 1: What are the labeled data points? References? Also, 'Engine worse condition' is still an odd way of putting it, as well as 'Lower limit of engine condition', how about ''Engine conditions at highest rotor speeds' and 'Engine**

conditions at lowest rotor speeds', respectively (or similar)?

In the revised caption of Figure 1, all the labeled data points are illustrated. The references corresponding to all the labeled data points are indicated in the Figure legends. The "Engine worse condition" is changed to "Engine conditions at highest rotor speeds and density ratios". The 'Lower limit of engine condition' is changed to "Engine conditions at lowest rotor speeds and density ratios".

Thank you for the suggestions.

3. **Figure 2: Please explain all parts of the Figure in the legend, including the top diagram and the graph at the left.**

Thank you for this suggestion. As we explained for comment 1, the legend of Figure 2 is revised as below to illustrate the plots at the top, the lower left and the lower right portions.

Figure 2. Typical heat loss coefficients (h_{loss}) at various rotating speeds[30] using the trapezoidal twin-pass rib-roughened rotating channel as an illustrative example. The top portion depicts the constructional details of the rotating test module. The slope of each data trend constituting by the heat loss flux against wall-to-ambient temperature difference shown in the left lower portion reveals the heat loss coefficient at the specific rotating speed. By correlating the heat loss coefficients detected at all the rotating speed tested, the generated heat loss correlation typified by the right lower plot is incorporated into the data processing program for Nu accountancy. The data range indicated in the lower right plot indicates the range of experimental uncertainties for h_{loss}[30].

4. Figure 2: What is the 'data range'? 'Range' in the statistical sense (i.e., the top and bottom of the error bars are the largest and smallest values), or something else like standard deviation?

The data range indicated in the lower right plot represents the range of experimental uncertainties for h_{loss}[30]. Thus, the explanation for such data range is added in the caption of Figure 2. Thank you.

Figure 2. Typical heat loss coefficients (h_{loss}) at various rotating speeds[30] using the trapezoidal twin-pass rib-roughened rotating channel as an illustrative example. The top portion depicts the constructional details of the rotating test module. The slope of each data trend constituting by the heat loss flux against wall-to-ambient temperature difference shown in the left lower portion reveals the heat loss coefficient at the specific rotating speed. By correlating the heat loss coefficients detected at all the rotating speed tested, the generated heat loss correlation typified by the right lower plot is incorporated into the data processing program for Nu accountancy. The data range indicated in the lower right plot indicates the range of experimental uncertainties for h_{loss}[30].

5. **Figure 3: Please explain the diagram at top more fully (in the legend as well). What are the dotted lines? What are the colored circles? What are A and A'? What does '5 mm' indicate, and what are the other dimensions? What are the wavy lines going through the module?**

Thank you for the comment. The unnecessary dotted lines are removed. The only dotted line indicates the location of AA' section. The colored circles are removed. As

indicated in the revised Fig. 3, the 5mm is the height of S-rib. The other dimensions are removed. The wavy lines going through the module are indicated as the longitudinal S-ribs in the revised Figure 3.
The revised Fig. 3 along with its modified caption are depicted as below.

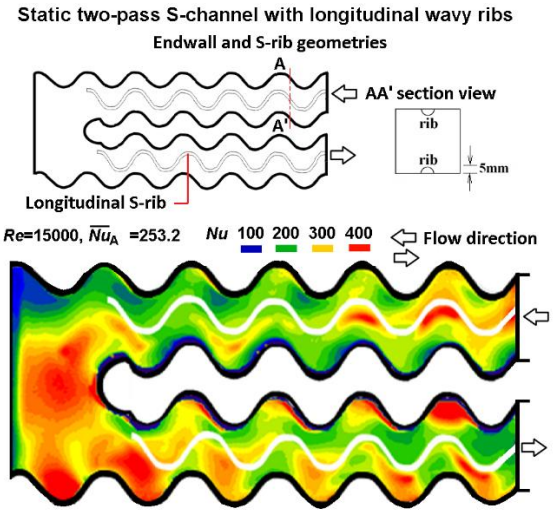

Figure 3. Local Nusselt number distribution of the static twin-pass S-channel roughened by curly ribs at Re=15000 measured by present infrared thermography method. The top diagram depicts the endwall of two-pass wavy channel and the longitudinal S-ribs. As indicated by the AA' section view, the pair of longitudinal S-ribs is in-lined arranged on two opposite channel endwalls. In the detailed distribution of Nusselt number over the two-pass wavy endwall shown as the lower plot, the Nu data along the two longitudinal S-ribs are discarded due to the wall conduction effects on the distributions of heat-flux and wall-temperature.

6. Figure 5: Please explain the lines and how well they fit in the Legend.
Thank you for the comment. The responses to this comment are included in the revised caption of Figure 5 as follows:

Figure 5. Examples demonstrating the uncoupled Ro effect from Bu impact on heat transfer properties of rotating channel[32,33]. Each Bu-driven Nu/Nu_0 variation is obtained at the fixed Ro and correlated as a linear function of Bu as indicated by the straight line in each plot. The correlation coefficients of these fitted lines fall between 0.96 and 1.02. The extrapolation of the Nu/Nu_0 data trend toward $Bu \rightarrow 0$ along each fitted line reveals the Nu/Nu_0 ratio at the tested Ro. The magnitude and slope of each Bu-driven Nu/Nu_0 data trend disclose the manners of buoyancy effect on heat transfer performances. The magnitudes of the slopes represent the degrees of Bu impact on Nu/Nu_0. The positive and negative slopes respectively reflect the improving and impairing buoyancy impact on heat transfer levels.

7. Figure 6: ‘trasnfer’ is a typo. Also, please explain the dotted lines in the legend.

Thank you. This typo is corrected in the revised Figure 6.

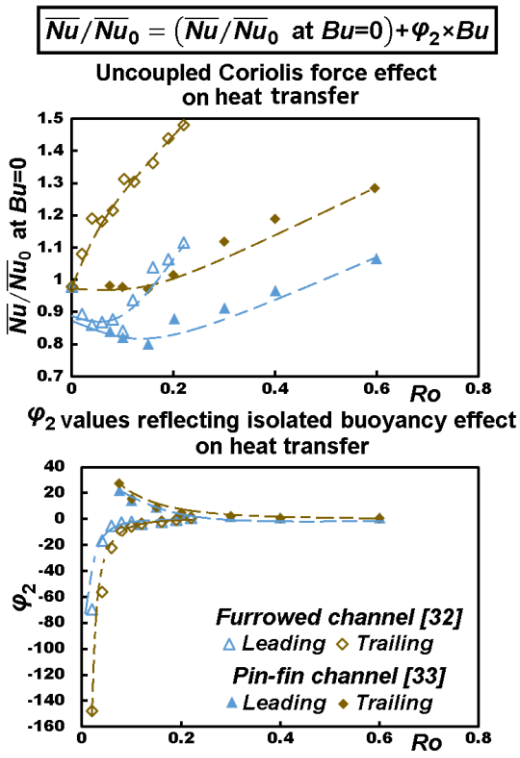

8. Figures 5/6: It looks like ref. 33 should also be cited in the Legends to these figures.
All the results compared in Figs. 5 and 6 are re-plotted as an attempt to demonstrate the differential Bu impacts on the heat transfer properties of the rotating channels with furrowed ednwalls[32] and pin-fins[33]. Thus, Figures 5 and 6 are the new plots. The ref. 33 are added in the Figure caption.

ELSEVIER LICENSE
TERMS AND CONDITIONS

Mar 15, 2018

This Agreement between S.W. W Chang ("You") and Elsevier ("Elsevier") consists of your license details and the terms and conditions provided by Elsevier and Copyright Clearance Center.

License Number	4310481244582
License date	Mar 15, 2018
Licensed Content Publisher	Elsevier
Licensed Content Publication	International Journal of Heat and Mass Transfer
Licensed Content Title	Thermal performance of radially rotating two-pass S-shaped zig-zag channel
Licensed Content Author	Shyy Woei Chang,Pey-Shey Wu,Chuan-Sheng Chen,Chien-Chou Weng,Yu-Ru Jiang,Shih-Hao Shih
Licensed Content Date	Dec 1, 2017
Licensed Content Volume	115
Licensed Content Issue	n/a
Licensed Content Pages	21
Start Page	1011
End Page	1031
Type of Use	reuse in a journal/magazine
Requestor type	author of new work
Intended publisher of new work	Other
Portion	figures/tables/illustrations
Number of figures/tables/illustrations	2
Format	both print and electronic
Are you the author of this Elsevier article?	Yes

Will you be translating?	Yes, including English rights
Number of languages	1
Languages	English
Original figure numbers	Figures 4, 5
Title of the article	An experimental method to uncouple effects of Coriolis force and rotating buoyancy on full-field heat transfer property of a rotating channel
Publication new article is in	Journal of Visualized Experiments
Publisher of the new article	Other
Author of new article	Shyy Woei Chang, Hong-Da Shen, Kuo-Ching Yu
Expected publication date	Sep 2018
Estimated size of new article (number of pages)	5
Requestor Location	S.W. W Chang No. 1, University Road, Tainan City Tainan, 701 Taiwan Attn: Prof. Shyy Chang
Publisher Tax ID	GB 494 6272 12
Total	0.00 USD
Terms and Conditions	

INTRODUCTION

1. The publisher for this copyrighted material is Elsevier. By clicking "accept" in connection with completing this licensing transaction, you agree that the following terms and conditions apply to this transaction (along with the Billing and Payment terms and conditions established by Copyright Clearance Center, Inc. ("CCC"), at the time that you opened your Rightslink account and that are available at any time at http://myaccount.copyright.com).

GENERAL TERMS

2. Elsevier hereby grants you permission to reproduce the aforementioned material subject to the terms and conditions indicated.

3. Acknowledgement: If any part of the material to be used (for example, figures) has appeared in our publication with credit or acknowledgement to another source, permission must also be sought from that source. If such permission is not obtained then that material may not be included in your

publication/copies. Suitable acknowledgement to the source must be made, either as a footnote or in a reference list at the end of your publication, as follows:
"Reprinted from Publication title, Vol /edition number, Author(s), Title of article / title of chapter, Pages No., Copyright (Year), with permission from Elsevier [OR APPLICABLE SOCIETY COPYRIGHT OWNER]." Also Lancet special credit - "Reprinted from The Lancet, Vol. number, Author(s), Title of article, Pages No., Copyright (Year), with permission from Elsevier."
4. Reproduction of this material is confined to the purpose and/or media for which permission is hereby given.
5. Altering/Modifying Material: Not Permitted. However figures and illustrations may be altered/adapted minimally to serve your work. Any other abbreviations, additions, deletions and/or any other alterations shall be made only with prior written authorization of Elsevier Ltd. (Please contact Elsevier at permissions@elsevier.com). No modifications can be made to any Lancet figures/tables and they must be reproduced in full.
6. If the permission fee for the requested use of our material is waived in this instance, please be advised that your future requests for Elsevier materials may attract a fee.
7. Reservation of Rights: Publisher reserves all rights not specifically granted in the combination of (i) the license details provided by you and accepted in the course of this licensing transaction, (ii) these terms and conditions and (iii) CCC's Billing and Payment terms and conditions.
8. License Contingent Upon Payment: While you may exercise the rights licensed immediately upon issuance of the license at the end of the licensing process for the transaction, provided that you have disclosed complete and accurate details of your proposed use, no license is finally effective unless and until full payment is received from you (either by publisher or by CCC) as provided in CCC's Billing and Payment terms and conditions. If full payment is not received on a timely basis, then any license preliminarily granted shall be deemed automatically revoked and shall be void as if never granted. Further, in the event that you breach any of these terms and conditions or any of CCC's Billing and Payment terms and conditions, the license is automatically revoked and shall be void as if never granted. Use of materials as described in a revoked license, as well as any use of the materials beyond the scope of an unrevoked license, may constitute copyright infringement and publisher reserves the right to take any and all action to protect its copyright in the materials.
9. Warranties: Publisher makes no representations or warranties with respect to the licensed material.
10. Indemnity: You hereby indemnify and agree to hold harmless publisher and CCC, and their respective officers, directors, employees and agents, from and against any and all claims arising out of your use of the licensed material other than as specifically authorized pursuant to this license.
11. No Transfer of License: This license is personal to you and may not be sublicensed, assigned, or transferred by you to any other person without publisher's written permission.
12. No Amendment Except in Writing: This license may not be amended except in a writing signed by both parties (or, in the case of publisher, by CCC on publisher's behalf).

13. Objection to Contrary Terms: Publisher hereby objects to any terms contained in any purchase order, acknowledgment, check endorsement or other writing prepared by you, which terms are inconsistent with these terms and conditions or CCC's Billing and Payment terms and conditions. These terms and conditions, together with CCC's Billing and Payment terms and conditions (which are incorporated herein), comprise the entire agreement between you and publisher (and CCC) concerning this licensing transaction. In the event of any conflict between your obligations established by these terms and conditions and those established by CCC's Billing and Payment terms and conditions, these terms and conditions shall control.
14. Revocation: Elsevier or Copyright Clearance Center may deny the permissions described in this License at their sole discretion, for any reason or no reason, with a full refund payable to you. Notice of such denial will be made using the contact information provided by you. Failure to receive such notice will not alter or invalidate the denial. In no event will Elsevier or Copyright Clearance Center be responsible or liable for any costs, expenses or damage incurred by you as a result of a denial of your permission request, other than a refund of the amount(s) paid by you to Elsevier and/or Copyright Clearance Center for denied permissions.

LIMITED LICENSE

The following terms and conditions apply only to specific license types:
15. **Translation**: This permission is granted for non-exclusive world **English** rights only unless your license was granted for translation rights. If you licensed translation rights you may only translate this content into the languages you requested. A professional translator must perform all translations and reproduce the content word for word preserving the integrity of the article.
16. **Posting licensed content on any Website**: The following terms and conditions apply as follows: Licensing material from an Elsevier journal: All content posted to the web site must maintain the copyright information line on the bottom of each image; A hyper-text must be included to the Homepage of the journal from which you are licensing at http://www.sciencedirect.com/science/journal/xxxxx or the Elsevier homepage for books at http://www.elsevier.com; Central Storage: This license does not include permission for a scanned version of the material to be stored in a central repository such as that provided by Heron/XanEdu. Licensing material from an Elsevier book: A hyper-text link must be included to the Elsevier homepage at http://www.elsevier.com . All content posted to the web site must maintain the copyright information line on the bottom of each image.

Posting licensed content on Electronic reserve: In addition to the above the following clauses are applicable: The web site must be password-protected and made available only to bona fide students registered on a relevant course. This permission is granted for 1 year only. You may obtain a new license for future website posting.
17. **For journal authors:** the following clauses are applicable in addition to the above:
Preprints:

A preprint is an author's own write-up of research results and analysis, it has not been peer-reviewed, nor has it had any other value added to it by a publisher (such as formatting, copyright, technical enhancement etc.).
Authors can share their preprints anywhere at any time. Preprints should not be added to or enhanced in any way in order to appear more like, or to substitute for, the final versions of articles however authors can update their preprints on arXiv or RePEc with their Accepted Author Manuscript (see below).
If accepted for publication, we encourage authors to link from the preprint to their formal publication via its DOI. Millions of researchers have access to the formal publications on ScienceDirect, and so links will help users to find, access, cite and use the best available version. Please note that Cell Press, The Lancet and some society-owned have different preprint policies. Information on these policies is available on the journal homepage.
Accepted Author Manuscripts: An accepted author manuscript is the manuscript of an article that has been accepted for publication and which typically includes author-incorporated changes suggested during submission, peer review and editor-author communications.
Authors can share their accepted author manuscript:

- immediately
    - via their non-commercial person homepage or blog
    - by updating a preprint in arXiv or RePEc with the accepted manuscript
    - via their research institute or institutional repository for internal institutional uses or as part of an invitation-only research collaboration work-group
    - directly by providing copies to their students or to research collaborators for their personal use
    - for private scholarly sharing as part of an invitation-only work group on commercial sites with which Elsevier has an agreement
- After the embargo period
    - via non-commercial hosting platforms such as their institutional repository
    - via commercial sites with which Elsevier has an agreement

In all cases accepted manuscripts should:

- link to the formal publication via its DOI
- bear a CC-BY-NC-ND license - this is easy to do
- if aggregated with other manuscripts, for example in a repository or other site, be shared in alignment with our hosting policy not be added to or enhanced in any way to appear more like, or to substitute for, the published journal article.

Published journal article (JPA): A published journal article (PJA) is the definitive final record of published research that appears or will appear in the journal and embodies all value-adding publishing activities including peer review co-ordination, copy-editing, formatting, (if relevant) pagination and online enrichment.

Policies for sharing publishing journal articles differ for subscription and gold open access articles:

Subscription Articles: If you are an author, please share a link to your article rather than the full-text. Millions of researchers have access to the formal publications on ScienceDirect, and so links will help your users to find, access, cite, and use the best available version.

Theses and dissertations which contain embedded PJAs as part of the formal submission can be posted publicly by the awarding institution with DOI links back to the formal publications on ScienceDirect.

If you are affiliated with a library that subscribes to ScienceDirect you have additional private sharing rights for others' research accessed under that agreement. This includes use for classroom teaching and internal training at the institution (including use in course packs and courseware programs), and inclusion of the article for grant funding purposes.

Gold Open Access Articles: May be shared according to the author-selected end-user license and should contain a CrossMark logo, the end user license, and a DOI link to the formal publication on ScienceDirect.

Please refer to Elsevier's posting policy for further information.

18. **For book authors** the following clauses are applicable in addition to the above: Authors are permitted to place a brief summary of their work online only. You are not allowed to download and post the published electronic version of your chapter, nor may you scan the printed edition to create an electronic version. **Posting to a repository:** Authors are permitted to post a summary of their chapter only in their institution's repository.

19. **Thesis/Dissertation**: If your license is for use in a thesis/dissertation your thesis may be submitted to your institution in either print or electronic form. Should your thesis be published commercially, please reapply for permission. These requirements include permission for the Library and Archives of Canada to supply single copies, on demand, of the complete thesis and include permission for Proquest/UMI to supply single copies, on demand, of the complete thesis. Should your thesis be published commercially, please reapply for permission. Theses and dissertations which contain embedded PJAs as part of the formal submission can be posted publicly by the awarding institution with DOI links back to the formal publications on ScienceDirect.

Elsevier Open Access Terms and Conditions

You can publish open access with Elsevier in hundreds of open access journals or in nearly 2000 established subscription journals that support open access publishing. Permitted third party re-use of these open access articles is defined by the author's choice of Creative Commons user license. See our open access license policy for more information.

Posting or linking by commercial companies for use by customers of those companies.

20. **Other Conditions**:

v1.9

Thank you for your order!

Dear Prof. Shyy Chang,

Thank you for placing your order through Copyright Clearance Center's RightsLink® service.

Order Summary

Licensee:	S.W. W Chang
Order Date:	Mar 15, 2018
Order Number:	4310481244582
Publication:	International Journal of Heat and Mass Transfer
Title:	Thermal performance of radially rotating two-pass S-shaped zig-zag channel
Type of Use:	reuse in a journal/magazine
Order Total:	0.00 USD

View or print complete details of your order and the publisher's terms and conditions.

Sincerely,

Copyright Clearance Center

How was your experience? Fill out this survey to let us know.

Tel: +1-855-239-3415 / +1-978-646-2777
customercare@copyright.com
https://myaccount.copyright.com